



# Benthos as a key driver of morphological change in coastal regions

Peter Arlinghaus<sup>1</sup>, Corinna Schrum<sup>1,2</sup>, Ingrid Kröncke<sup>3,4</sup>, and Wenyan Zhang<sup>1</sup>

<sup>1</sup>Institute of Coastal Systems – Analysis and Modeling, Helmholtz-Zentrum Hereon, Geesthacht, Germany

<sup>2</sup>Center for Earth System Sustainability, Institute of Oceanography, Universität Hamburg, Hamburg, Germany

<sup>3</sup>Institute for Chemistry and Biology of the Marine Environment (ICBM),  
Carl von Ossietzky University, Oldenburg, Germany

<sup>4</sup>Department for Marine Research, Senckenberg am Meer, Wilhelmshaven, Germany

**Correspondence:** Peter Arlinghaus (peter.arlinghaus@hereon.de) and Wenyan Zhang (wenyan.zhang@hereon.de)

Received: 14 June 2023 – Discussion started: 12 July 2023

Revised: 13 February 2024 – Accepted: 6 March 2024 – Published: 22 April 2024

**Abstract.** Benthos has long been recognized as an important factor influencing local sediment stability, deposition, and erosion rates. However, its role in long-term (annual to decadal scale) and large-scale coastal morphological change remains largely speculative. This study aims to derive a quantitative understanding of the importance of benthos in the morphological development of a tidal embayment (Jade Bay) as representative of tidal coastal regions. To achieve this, we first applied a machine-learning-aided species abundance model to derive a complete map of benthos (functional groups, abundance, and biomass) in the study area, based on abundance and biomass measurements. The derived data were used to parameterize the benthos effect on sediment stability, erosion rates and deposition rates, erosion and hydrodynamics in a 3-dimensional hydro-eco-morphodynamic model, which was then applied to Jade Bay to hindcast the morphological and sediment change for 2000–2009. Simulation results indicate significantly improved performance with the benthos effect included. Simulations including benthos show consistency with measurements regarding morphological and sediment changes, while abiotic drivers (tides, storm surges) alone result in a reversed pattern in terms of erosion and deposition contrary to measurement. Based on comparisons among scenarios with various combinations of abiotic and biotic factors, we further investigated the level of complexity of the hydro-eco-morphodynamic models that is needed to capture long-term and large-scale coastal morphological development. The accuracy in the parameterization data was crucial for increasing model complexity. When the parameterization uncertainties were high, the increased model complexity decreased the model performance.

## 1 Introduction

Benthos includes flora such as seagrass, kelp, and salt marsh species, which predominately stabilize sediment (Corenblit et al., 2011; Zhang et al., 2012, 2015), and fauna with more complex behaviors that can stabilize or destabilize sediment (Backer et al., 2010). Benthic in- and epifauna actively rework sediment in order to increase the availability of resources for themselves (Jones et al., 1994; Meadows et al., 2012) and play a critical role in modifying sediment prop-

erties such as grain size, porosity, permeability, and stability at local scales in coastal environments (Backer et al., 2010; Arlinghaus et al., 2021; Murray et al., 2008).

The different behaviors of benthos and the consequent impacts on sediment have been described in numerous studies and literature reviews (Arlinghaus et al., 2021; Andersen and Pejrup, 2011; le Hir et al., 2007). Major benthos behaviors include biomixing (Lindqvist et al., 2016; Queiros et al., 2013; Meyer et al., 2019; Weinert et al., 2022), bioirrigation (Wrede et al., 2017), bio-deposition and bio-resuspension

(Cozzoli et al., 2019; Graf and Roseberg, 1997), faecal pellet production (Andersen and Pejrup, 2011; Grant and Daborn, 1994; Troch et al., 2008), and biofilm stabilization (Le Hir et al., 2007; Stal, 2010). All of the ways in which benthos changes and modifies the sediment directly or indirectly are termed bioturbation (Meysman et al., 2007). The impacts of bioturbation on sediments can individually or accumulatively lead to dramatic local morphological changes, as demonstrated by defaunation experiments (Volkenborn and Reise, 2006; Volkenborn et al., 2009; Montserrat et al., 2008). However, most studies are limited to small temporal and spatial scales, and it remains unclear whether such small-scale benthos–sediment interactions could affect long-term (annual to decadal scale) and large-scale (kilometer to basin scale) coastal morphological change.

Over the past 3 decades, increasing efforts have been dedicated to upscaling the impacts of benthos–sediment interactions to larger scales through the use of numerical modeling (Arlinghaus et al., 2021). Results indicate that benthos can induce erosion that is in the same order of magnitude as hydrodynamics (Wood and Widdows, 2002; Lumborg et al., 2006; Arlinghaus et al., 2022) and can cause the redistribution of sediments at large spatial scales, e.g., across tidal basins (Borsje et al., 2008) and coastal bays (Nasermoaddeli et al., 2017). Fine-grained, muddy sediments are especially sensitive to benthos impacts (Paarlberg et al., 2005; Knaapen et al., 2003; Smith et al., 1993). However, almost all modeling studies applied at large scales are limited to qualitative results (Arlinghaus et al., 2021). Following the concept of Desjardins et al. (2018), numerical models can be categorized into three types corresponding to successive development stages, namely explorative, explanatory, and predictive models. In explorative hydro-eco-morphodynamic models, the processes and their parameterizations are varied within a certain range, creating an ensemble of possible final states to estimate and explore the impact range of a driver, e.g., benthos, on morphological evolution. In explanatory models, a certain final state is known, and the model parameters are tuned in order to hindcast the change in the system from an initial state to the final state as accurately as possible so that the simulation results can be used to understand the magnitude and relative importance of the involved processes contributing to the final state. Most hydro-eco-morphodynamic models are still at the explorative stage and have yet to reach the explanatory stage, and the reasons are manifold. In general, benthic physical and biological processes are highly complex, involving many feedback loops and boundary conditions with large variability (Oreskes et al., 1994; French et al., 2015; Larsen et al., 2016); e.g., many biophysical functions such as the formation of biofilm and its impact on sediment stability remain still poorly understood (Stal, 2010; Van Colen et al., 2014; Chen et al., 2017). Interactions between different functional groups of benthos and between benthos and seabed morphology are important in coastal morphodynamics (Murray et al., 2008; Marani et al., 2010; Corenblit

et al., 2011; Reinhardt et al., 2010; Zarnetske et al., 2017) but have rarely been incorporated in large-scale modeling (Arlinghaus et al., 2022; Brückner et al., 2021). Shortage of continuous field monitoring data (e.g., mapping of benthos and seabed morphology) with long-term coverage impedes a process-based understanding and mathematical description of benthic biophysical functions (Arlinghaus et al., 2021).

Explanatory models represent an intermediate stage of model development from exploratory toward predictive modeling (Desjardins et al., 2018). This study presents an effort to this end in hydro-eco-morphodynamic modeling. For this purpose, Jade Bay, a tidal embayment located in the German Wadden Sea, was chosen to test the model. The reason for choosing Jade Bay is that extensive datasets for both morphological evolution and biological parameters are available for the area, providing a unique opportunity for an explanatory modeling investigation.

Tidal embayments such as Jade Bay are commonly found worldwide (Haas et al., 2018). They are among the most productive ecosystems on the Earth's surface, providing a variety of ecosystem functions (Mitsch and Gosselink, 2007) and serving as important habitats for marine life-forms (Levin et al., 2001). On the other hand, they are commonly utilized for fishing, navigation, and tourism and endure strong population pressure (Duong et al., 2016). Depending on the effects of different biotic and/or abiotic drivers, tidal embayments may persist for centuries, be filled up or closed (Haas et al., 2018), or be drowned (Plater and Kirby, 2011). Thus, understanding the morphodynamics of these systems is crucial for coastal mitigation and adaptation in response to climate change and human use.

In this study, an elaborate hydro-eco-morphodynamic model is used to hindcast the morphological development of Jade Bay from 2001 to 2009. Jade Bay benthos data include infauna (> 0.5 mm) and seagrass. By incorporating the impacts of these two types of benthos, we aim to address the following specific questions:

1. To what extent does benthos account for the observed changes in the morphology and sediment composition in the study area?
2. What are the individual and combined impacts of different functional groups on morphological development?

## 2 Study area

Jade Bay is located in the inner part of the German Wadden Sea and connected to the outer part through a deep (> 15 m) tidal inlet (Fig. 1). The tidal inlet and Jade Bay have a combined length of approx. 36 km and vary in width between 4 and 15 km, covering around 370 km<sup>2</sup>, with 160 km<sup>2</sup> inside the bay, about 60 % of which is comprised of tidal flats (Lang, 2003). Jade Bay is a meso-tidal system with a tidal range of ca 3.7 m (Svenson et al., 2009). The water depth

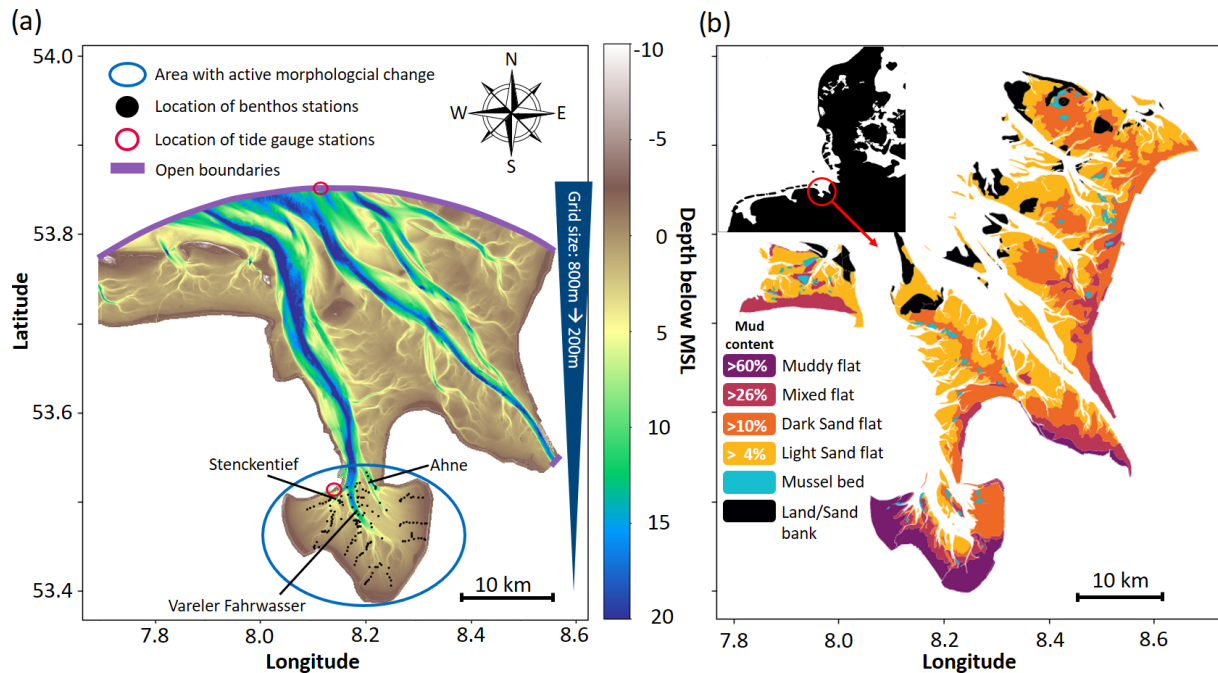


**Figure 1.** (a) Computational domain and its open boundary, including the initial morphology at 2001, the location of benthos data, and tide gauge stations. (b) Distribution of sediment types, including land and mussel beds (Meyer and Ragutski, 1999).

of the main channel reaches up to 20 m below the mean sea level. The main channel penetrates Jade Bay and branches into three major basin channels which are permanently inundated (Stenckentief, Vareler Fahrwasser, and Ahne; see Fig. 1a). The intertidal area has a mean water depth of 2.07 m during high tide (Von Seggern, 1980). Tidal currents transport an average volume of  $0.4 \text{ km}^3$  per tidal cycle with speeds exceeding  $1.5 \text{ ms}^{-1}$  in the channels (Götschenberg and Kahlfeld, 2008). A training wall guides tidal currents, leading to finer sediments towards the western and southern parts of the bay (Linke, 1939; Götschberg and Kahlfeld, 2008). The central part of the channel is characterized by medium to coarse sands, while towards the banks, fine sands with increasing mud content are found (Reineck and Singh, 1967). Three bed types can be distinguished: sandflats, mudflats, and mixed. The bay is inhabited by abundant benthic fauna and seagrass meadows (*Zostera noltii*). In terms of biomass, the most abundant organisms are Bivalvia (*Cerastoderma edule* and *Macoma balthica*), Gastropoda (*Peringia ulvae*), and Polychaetes (*Arenicola marina*, *Hediste diversicolor*, and *Tubificoides benedii*), with a spatially averaged biomass of  $20 \text{ g C m}^{-2}$  according to Schückel et al. (2015b). Typical values of benthic biomass range between  $1\text{--}100 \text{ g C m}^{-2}$  in the Wadden Sea (Beukema, 1974; Reise et al., 1994; Beukema and Dekker, 2020).

### 3 Methods

#### 3.1 Machine-learning-aided mapping of macrobenthos

According to the impacts of benthos on sediment dynamics and to achieve an appropriate level of model complexity, benthos are sorted into functional groups. A functional group comprises species from different taxa that impact their environment in similar ways (Kristensen et al., 2012). In this study, benthos is categorized into four major functional groups, namely bioturbators, stabilizers, accumulators, and seagrass. Bioturbators and accumulators consist of macrobenthos, while stabilizers are represented by a biofilm which is mainly assembled by microphytobenthos (MPB) of all contributing species. The seagrass present in Jade Bay belongs to the species *Zostera noltii* (Adolph, 2010).

The existing field dataset provides macrobenthos abundance in the inter-tidal area and abundance plus biomass for the subtidal area at 160 stations in Jade Bay (Senckenberg; Schückel and Kröncke, 2013; Schückel et al., 2015a). Based on the intertidal abundance values and biomass averages from the subtidal measurements, the intertidal biomass could be calculated (Fig. 2b–f). The total measured biomass in Jade Bay is dominated by a few species which are widely distributed in the area. Since the metabolic rate of bioturbators is a useful indicator for bioturbation intensity (Cozzoli et al., 2019) which scales with biomass, we focus on five dominant species which make up 95% of benthos biomass in the area, namely the mussels *Cerastoderma edule* (accumulator) and *Macoma balthica* (accumulator and bioturbator),

the snail *Peringia ulvae* (biomixer), and the worms *Hediste diversicolor* (biomixer) and *Tubificoides benedii* (biomixer). Complete mapping of benthos for the entire Jade Bay is done by extrapolation from 160 field stations. Species distribution modeling (SDM) is commonly used for this purpose, which produces probabilities of species occurrence. Various methods have been applied, spanning from statistical methods to machine learning (Waldock et al., 2021). Species abundance modeling (SAM) is developed from SDM and has an increased solution space, since the output represents decimal values covering the whole range of measured abundance spectrum or biomass spectrum, respectively. Existing studies show the best results when using decision trees (Luan et al., 2020; Waldock et al., 2021). For this reason, we adopted a decision-tree-based SAM to generate a complete map of benthos in the study area. A detailed description of the method and an analysis of the applied dataset are provided in the Supplement.

Six predictor variables at the stations, namely temperature, salinity, chl *a* content, inundation time, shear stress, and mud content were used. The first three were derived via image analysis of the plots from Jade Bay SDM results by Singer et al. (2016), and the latter three were extracted from the hydrodynamic model results. Abundance and biomass of the five dominant species are target variables. For each of the species, a separate regression tree model was run for Jade Bay area. In addition, the SAM was extended to cover the inner and outer Jade. However, in this area there are no benthos field data for model validation, and the number of predictor variables is reduced to three (mud content, shear stress, and inundation time). Based on the field data, two SAMs were applied for each species, with one for abundance and one for biomass, in order to calculate the mean individual biomass which is needed for the parameterization of benthos impacts on sediment. We used 90 % of the species data points for model training and the remaining 10 % to test the model performance.

Although the field dataset of benthos abundance and biomass is uniquely comprehensive for a tidal basin in the Wadden Sea, seasonal variations were not covered. To take into account seasonal variations in the benthos impact, a simple sinusoidal function describing the change in the biomass and related bioturbation intensity (see details in Sect. 3.2.1) was used in some of the model experiments described in Table 3.

### 3.2 Mathematical description of benthos impact

Impacts of benthos on sediment are formulated through scaling functions between benthos abundance/biomass and model parameters for sediment dynamics, namely the critical shear stress for erosion  $\tau_c$  (Pa), the erosion rate  $E_r$  ( $\text{kg m}^{-2} \text{s}^{-1}$ ), the sediment-settling velocity  $W_{\text{sed}}$  ( $\text{mm s}^{-1}$ ), and hydrodynamic parameters for turbulence and bottom shear stress. For sediment erosion, the general approaches

by Knaapen et al. (2003) for  $\tau_c$  and Paarlberg et al. (2005) for  $\tau_c$  and  $E_r$  are applied. An abiotic critical shear stress for erosion  $\tau_c^0$  and the erosion rate  $E_r^0$  is scaled by dimensionless biomixing functions  $p_d$ ,  $g_d$  and stabilization functions  $p_s$ ,  $g_s$ , respectively, which depend on the abundance  $A$  (number of individuals) and biomass  $B$  (milligrams of ash-free dry weight (AFDW)) of these two functional groups:

$$\tau_c = \tau_c^0 \cdot p_d(B, A) \cdot p_s(B, A), \quad (1)$$

$$E_r = E_r^0 \cdot g_d(B, A) \cdot g_s(B, A). \quad (2)$$

Changes in hydrodynamics by the effect of seagrass are incorporated using the submerged aquatic vegetation model (SAV) of SCHISM (Zhang et al., 2016), and changes in  $W_{\text{sed}}$  by the effect of accumulators are applied according to a filter-feeder ingestion rate model (US Army Corps of Engineers, 2000). Both are explained in the following sections. No direct control between different functional groups is considered in the presented simulations.

#### 3.2.1 Biomixers

The main effect of biomixers is sediment destabilization. However, biomixing macrobenthos can also increase sediment stability in certain conditions of the metabolic rate, bottom shear stress, and sediment composition (Cozzoli et al., 2019), which is attributed to hardening of mucus excreted during locomotion (Orvain, 2002; Le Hir et al., 2007). In our model, the formulae from Cozzoli et al. (2019) are adopted to relate biomixing effect with the overall metabolic rate  $M_{\text{TOT}}$  (mW). In this study, measurements of the total eroded sediment per unit area in a given time,  $R_{\text{TOT}}$  ( $\text{g m}^{-2}$ ), were taken. Assuming that the erosion rate ( $\text{kg m}^{-2} \text{s}^{-1}$ ) over the given time is constant, it can be described by

$$R_{\text{TOT}} = \frac{a}{1 + \exp\left(\frac{b - \tau_b}{c}\right)}, \quad (3)$$

where the factors  $a$  ( $\text{g m}^{-2}$ ) and  $b$  (Pa) are related to  $M_{\text{TOT}}$  and  $B$ ,  $c$  (Pa) is an empirical constant, and  $\tau_b$  is the bottom shear stress. In order to calculate  $M_{\text{TOT}}$ , measurements from Cozzoli et al. (2019) (Table 1) are used to estimate the individual metabolic rate ( $M_{\text{Indv}}$  (mW)) from the individual biomass ( $B_{\text{Indv}}$  (milligrams of AFDW)):

$$M_{\text{Indv}} = 0.0067 \cdot B_{\text{Indv}}^{0.835}. \quad (4)$$

The SAM results for abundance and biomass are then used to calculate the mean individual biomass, which is fed into Eq. (4) to derive  $M_{\text{Indv}}$  and the total metabolic rate  $M_{\text{TOT}}$  by multiplying it with the abundance  $A$ . The derived value of  $M_{\text{TOT}}$  is then used to calculate the factors  $a$  and  $b$  under the biomixing impact ( $a_{\text{bio}}$  and  $b_{\text{bio}}$ ):

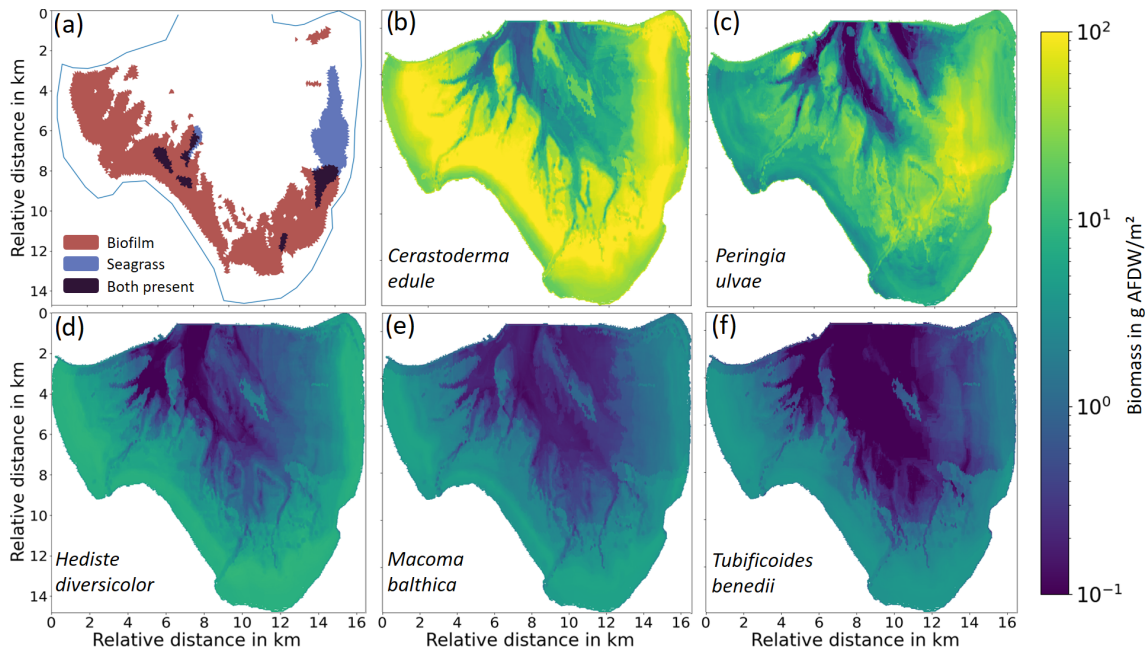


**Figure 2.** (a) Presence of stabilizers and seagrass according to Adolph (2010). (b–f) Modeled biomass distribution of the five dominant benthic faunal species.

$$a_{\text{bio}} = 41.67 \cdot (1 + M_{\text{TOT}})^{0.34} \cdot (1 + B_{\text{Indv}})^{-0.09}, \quad (5)$$

$$b_{\text{bio}} = 0.1 + 0.01 \cdot \log(1 + M_{\text{TOT}}). \quad (6)$$

The total eroded sediment under biomixing impact,  $R_{\text{TOT}}^{\text{bio}}$ , is calculated by feeding  $a_{\text{bio}}$  and  $b_{\text{bio}}$  into Eq. (3). The total eroded sediment under abiotic conditions  $R_{\text{TOT}}^0$  is calculated based on the formulation given in Cozzoli et al. (2019) and is used to derive the biomixing function  $g_d$ :

$$g_d = \frac{R_{\text{TOT}}^{\text{bio}}}{R_{\text{TOT}}^0}. \quad (7)$$

The other biomixing function  $p_d$  is calculated following Brückner et al. (2021), which is also based on the data from Cozzoli et al. (2019). Abiotic ( $\tau_c^0$ ) and biotic critical shear stress for erosion ( $\tau_c^{\text{bio}}$ ) are defined based on the respective  $\tau_b$  value at which a minimal erosion rate of  $25 \text{ g m}^{-2}$  is reached. This is done by converting Eq. (3) into

$$\tau_c = b - c \cdot \log\left(\frac{a - R_{25}}{R_{25}}\right). \quad (8)$$

$\tau_c^0$  is calculated using  $a_0$ ,  $b_0$ , and  $c_0$ , which are constants for the defaunated control experiments given in Table 1 in Cozzoli et al. (2019). For  $\tau_c^{\text{bio}}$ ,  $a_{\text{bio}}$ ,  $b_{\text{bio}}$ , and  $c_0$  are used.  $p_d$  is then calculated via

$$p_d = \frac{\tau_c^{\text{bio}}}{\tau_c^0}. \quad (9)$$

$g_d$  and  $p_d$  are calculated by adding up all biomixing species considered in the SAM. For Jade Bay, the derived values of  $g_d$  and  $p_d$  show a strong destabilizing effect on a vast part of the bay, especially on the tidal flats, while the subtidal area is mainly stabilized (Fig. S3).

Macrobenthic oxygen consumption rate may decrease by a factor of 10 during winter compared to summer (Glud et al., 2003; Renaud et al., 2007), and thus, biomixing intensity may also decrease accordingly. To account for this seasonal variability, a multiplication factor for  $M_{\text{TOT}}$  was introduced according to a sine function with a period of 1 year, reaching the maximum value of 1.0 in summer and the minimum value of 0.1 during winter.

### 3.2.2 Stabilizers

The stabilization functions  $p_s$  and  $g_s$  are related to biofilm, which is primarily built by microphytobenthos (MPB). According to measurements by le Hir et al. (2007) and Waeles et al. (2004), an increase in the critical shear stress for erosion ( $\tau_c$ ) by a factor of 4 ( $p_s = 4$ ) is implemented for the summer months (from June to September) when MPB is present. For the rest of the year, a factor of 1 is used because MPB is mostly not present in winter and thus has no effect ( $p_s = 1$ ). The erosion rate ( $E_r$ ) is assumed to be unaffected by MPB; thus,  $g_s$  is set to 1 as a constant.

**Table 1.** Data sources used for model initialization (Init.), parameterization (Param.), and model validation (Valid.).

Type	Use	Time	Description	Source/provider
Benthos	Init.	2009	Abundance and biomass at 160 field stations	Senckenberg; Kröncke, and Schückel (2013), Schückel et al. (2015a)
Benthos	Param.	–	Laboratory erosion measurements with different species at different densities	Cozzoli et al. (2019)
Benthos	Param.	–	Filter feeding rate for accumulators	U.S. Army Corps of Engineers (2000)
Benthos	Param.	–	Estimated MPB impact	Le Hir et al. (2007)
Benthos	Param.	–	Seagrass impact on hydrodynamics	SAV module of SCHISM, Adolph (2010)
Sediment	Init.	1996	Sediment map	Meyer and Ragutski (1999)
Sediment	Valid.	1996–2009	Map of sediment change	Ritzmann and Baumberg (2013)
Forcing: tides	Init.	2001–2009	Finite-element global ocean tide atlas	FES2014 Lyard et al. (2021)
Forcing: storms	Init.	2001–2009	Observed water elevation data at the gauge station Alte Weser Lighthouse	Wasserstraßen- und Schifffahrtsverwaltung des Bundes (WSV, 2023)
Water level	Valid.	2001–2009	Observation data at the gauge station Wilhelmshaven	Wasserstraßen- und Schifffahrtsverwaltung des Bundes (WSV, 2023)
Morphology	Init. + Valid.	2001–2009	High-resolution morphology of the German Bight	Sievers et al. (2020)

### 3.2.3 Accumulators

The presence of accumulators (mainly suspension and filter feeders) such as mussels effectively increases the settling velocity of sediment particles in the bottom water layer. The magnitude of resulting bio-deposition rate of sediments depends on the filtration rate and ingestion rate  $I$  ( $\text{L mg}^{-1}$ ) of accumulators, which scales with biomass  $B_{\text{acc}}$  ( $\text{mg AFDW m}^{-2}$ ). In this study, a simplified version of the filter-feeder model from the U.S. Army Corps of Engineers (2000), excluding the temperature effect, was applied. Sediment particle settling velocity in the bottom most water layer ( $W_{\text{sed}}$ ) is modified by

$$W_{\text{sed}} = W_{\text{sed}}^0 + I \cdot B_{\text{acc}}, \quad (10)$$

where  $W_{\text{sed}}^0$  represents the settling velocity without the effect of accumulators. Further details of the parameterization are provided in the Supplement.

### 3.2.4 Seagrass

The impact of seagrass is incorporated by an additional drag term in the Reynolds-averaged Navier–Stokes equation and an additional source term for turbulent kinetic energy and

mixing length, following the implementation of Cai (2018). The magnitude of these terms depends on the canopy height  $h$  (mm), stem diameter  $d$  (mm), stem density  $N$  ( $\text{m}^{-2}$ ), and drag coefficient for vegetation  $c_D$ . The parameters were chosen according to the vegetation cover and the common densities of *Z. noltii* in the German Wadden Sea (Adolph, 2010) and are listed in the model setup section (after Sect. 3.3). Seasonal change in the seagrass is not included in this study due to a lack of field data support for parameterization.

### 3.3 Hydro-eco-morphodynamic numerical model

The formulae for the benthos effect on sediment dynamics described in Sect. 3.2 are integrated into a 3-dimensional modeling system SCHISM (Zhang et al., 2016) to simulate hydro-eco-morphodynamics. SCHISM solves the Reynolds-averaged Navier–Stokes equation on an unstructured horizontal grid employing a semi-implicit Galerkin finite-element method (FEM). Vertical velocities and transport are computed with a finite-volume method (FVM) approach for a flexible number of vertical layers, allowing the transition between regions of different depth and resolution (Zhang and Baptista, 2008). Turbulence closure is implemented according to the  $k$ – $k\ell$  closure scheme described in Umlauf and Bur-

chard (2003). The original SCHISM framework includes a sediment module (SED3D; Pinto et al., 2012) which does not take into account the impacts of benthos. Sediment is divided into multiple classes, each with characteristic parameters including grain size, density, settling velocity, erosion rate, and critical shear stress for erosion. Cohesive and non-cohesive sediments are distinguished. Non-cohesive sediments (sands) can be transported in both suspension and bedload, depending on the shear stress and settling velocity, while cohesive sediment (clay, silt, and organic detritus) is transported in suspension. Transport of each pre-defined sediment class is computed independently.

### 3.4 Model setup for the study area

The model domain spans roughly from 53°23′ N 8°35′ E to 53°53′ N 7°46′ E (Fig. 1a). It is covered by unstructured triangular elements with a spatial resolution of approx. 800 m in the outer Jade Bay and an increasing resolution toward Jade Bay, with a resolution of approx. 200 m inside the bay. The vertical plane is divided into 11 sigma layers. The open boundary is forced by 15 tidal constituents (M2, K1, S2, O1, N2, P1, SA, K2, Q1, NU2, J1, L2, T2, MU2, and 2N2) extracted from the global ocean tide atlas FES2014 (Lyard et al., 2021), as well as observed storm surges which were implemented in terms of water level changes (see the Supplement). These changes are based on measurements at a gauge station (Alte Weser Lighthouse) located at the open boundary (Fig. 1a). Discharge is specified for the Weser River at the southeastern boundary of the modeling domain, according to Galbiati et al. (2008). Two sediment classes which are dominant in the study area (Fig. 1b) are included, namely fine sands with an initial settling velocity ( $W_{\text{sed}}^0$ ) of  $1 \text{ mm s}^{-1}$  and mud with an initial settling velocity ( $W_{\text{sed}}^0$ ) of  $0.02 \text{ mm s}^{-1}$ . A constant mud concentration of  $40 \text{ mg L}^{-1}$  is specified at the open boundary, according to Pleskachevsky et al. (2005). Seasonal variability in the suspended sediment concentration (SSC) at the open boundary was not implemented due to the lack of measurement data. Turbidity and sediment concentration measurements from Jade Bay typically cover one or a few points measured over one or a few tidal cycles (Götschenberg and Kahlfeld, 2008; Becker, 2011), while longer and larger-scale measurements were absent. SSC values in the presented simulations are in the same range as the measurements from Jade Bay (Becker, 2011) and comparable to another simulation study in Jade Bay (Kahlfeld and Schüttrumpf, 2006). A map of the simulated SSC is provided in the Supplement (Fig. S7).

Datasets from various sources are used to initialize, parameterize, and validate the model. A brief summary of these datasets is given in Table 1. The model is used to hindcast the change in the morphology and sediment composition in Jade Bay from July 2001 until December 2009. The measured morphology in 2001 serves as the initial condition. There are no sediment property measurements for the periods around

**Table 2.** Configuration of default model parameters for abiotic conditions.

Parameter	Configuration
$h$	25 cm
$d$	0.2 cm
$N$	$400 \text{ m}^{-2}$
$c_D$	1.13
$\tau_c^0$	0.2 Pa
$E_r^0$	$2 \times 10^{-5} \text{ s m}^{-1}$
$E_r^{10}$	$2 \times 10^{-4} \text{ s m}^{-1}$
$W_{\text{sed,mud}}^0$	$2 \times 10^{-5} \text{ m s}^{-1}$
$W_{\text{sed,sand}}^0$	$1 \times 10^{-3} \text{ m s}^{-1}$

2001; therefore, measured data from 1996 (Fig. 1b) were used to specify the initial mud and sand contents. Default model parameters representing abiotic conditions are listed in Table 2.

In order to disentangle the impacts of benthos, including the effect of individual functional groups and the combined effect of all functional groups and abiotic drivers on morphological and sediment change in the study area, a total of 27 different model experiments have been performed (Table 3). The experiments were designed to include different levels of complexity in the variability in the physical forcing (e.g., with and without storms) and benthos (e.g., with and without seasonality). In addition, an increased erosion rate was applied to some experiments that excluded bioturbators for comparability reasons. Bioturbators strongly enhance SSC, which leads to an increase in the impact of other functional groups such as accumulators. To achieve comparable SSC levels in simulations excluding bioturbators, the basic erosion rate ( $E_0$ ) was increased by a factor of 10 ( $E_{10}$ ), which helps to distinguish the effects of certain functional groups from scenarios with all benthic groups included.

## 4 Results

### 4.1 Mapping of benthos

To assess the performance of the decision-tree-based SAM, the measured data were split into training and validation datasets. The training dataset was used for training the model, and the validation dataset was checked against the resulting estimations of biomass and abundance. The performance of the SAM varies among the selected species. For the majority of the points, the estimated value deviates from the measured value by less than 20% (Fig. S2). Biomass and abundance distributions of all five species are shown in Fig. 2b–f.

For stabilizers, biofilm built by MPB is considered, which is only distinguished by its presence or absence in the field data. We applied a formulation relating the growth of MPB-based biofilm to the inundation period and mud content, fol-

**Table 3.** Model experiments are designed for a combination of different physical forcing and functional groups which are abbreviated as mix (biomixers), *acc* (accumulators), *sta* (stabilizers), *gra* (seagrass), all (inclusion of all functional groups), and *abio* (abiotic model run without consideration of any benthos effect). Seasonal variations in benthos impact are abbreviated as *no* (followed by the abbreviation of a specific functional group) if they were excluded or included. Hydrodynamic forcing excluding or including storm surges is abbreviated as T or TS, and a default erosion rate or an erosion rate scaled by a factor of 10 is abbreviated as 1 or 10. The experiments are named by combination according to the different model features, separated by an underscore, and read as modeled functional groups\_seasonality\_hydrodynamics\_erosion rate. For example, in the model experiment *acc\_acc\_TS\_10*, accumulators are the simulated functional group, seasonality of accumulators was considered, both tides and storm surges were considered hydrodynamic forcing, and the erosion rate was scaled by a factor of 10.

	E0	E0 + storm	E0 + storm + seasonality	E0 + storm + seasonality all	E10	E10 + storm	E10 + storm + seasonality
All benthos	all_no_T_1	all_no_TS_1	all_mix_TS_1	all_all_TS_1	–	–	–
Biomixers	mix_no_T_1	mix_no_TS_1	mix_mix_TS_1	–	–	–	–
Stabilizers	sta_no_T_1	sta_no_TS_1	sta_sta_TS_1	–	sta_no_T_10	sta_no_TS_10	sta_sta_TS_10
Accumulators	acc_no_T_1	acc_no_TS_1	acc_acc_TS_1	–	acc_no_T_10	acc_no_TS_10	acc_acc_TS_10
Seagrass	gra_no_T_1	gra_no_TS_1	–	–	gra_no_T_10	gra_no_TS_10	–
Abiotic drivers only	abio_no_T_1	abio_no_TS_1	–	–	abio_no_T_10	abio_no_TS_10	–

lowing the studies by Widdows and Brinsley (2002) and Daggers et al. (2020). In Jade Bay, only the western and southern parts are inhabited by extensive biofilms (Fig. 2a).

Seagrass distribution in Jade Bay is described for the years 2000–2008 in Adolph (2010), with vegetation density between 5%–40% for the dominant species *Zostera noltii* (Fig. 2a).

#### 4.2 Assessment of hydro-eco-morphodynamic model performance

Simulated time series of the water level in all experiments are quite similar and exhibit differences only during storm periods between the experiments with and without storms. A comparison with measured water level at a tide gauge station in Wilhelmshaven, which is located at the inlet of Jade Bay, shows a satisfactory model performance (Fig. 3). Taking the reference experiment *abio\_no\_TS\_10* as an example, the standard deviation is 1.34 m for the data measured at the gauge station compared to 1.33 m derived from model results. For the tide gauge station at the Alte Weser Lighthouse, the values are 1.03 and 0.99 m, respectively. The correlation coefficient between the modeled water elevation and measured data is 0.98 at Wilhelmshaven and 0.96 at Alte Weser station (Fig. 3b).

The simulated change in the sediment composition and morphology in all experiments is compared and evaluated. First, simulation results are evaluated against observed changes to rank the performance of the experiments. Then, the impact of individual functional groups and their combined effect is analyzed based on the model results. In addition, the level of complexity of hydro-eco-morphodynamic models that is needed to capture long-term and large-scale coastal morphological development is investigated.

In order to minimize the effect of uncertainty in measurements, only the grid cells where the measured morphological change exceeds the standard deviation of difference between

the 2001 and 2009 field data were chosen for the comparison in Fig. 4. Two indicators, namely the RMSE and the cosine similarity between the modeled and measured morphological change, were calculated for each of the experiments and are shown in Fig. 4.

The RMSE (Fig. 4a) shows the best model performance in the group of experiments (*all\_x*) which takes into account the combined effect of all benthos functional groups, followed by the group of experiments (*mix\_x*) which includes the effect of biomixers only. The experiments (*acc\_x*) which include only the accumulators show a better performance than the reference experiments (*abio\_x*) which consider only abiotic drivers, while the experiments which include only seagrass (*gra\_x*) or stabilizers (*sta\_x*) do not show noticeable improvement compared to abiotic scenarios. The difference in the RMSE between the model results with the best and the worst performance is about 15 cm, which is about 150% of the average and 35% of the standard deviation of morphological change for the entire Jade Bay from 2001 to 2009. It is worth noting that within the group of experiments (*all\_x*) which includes all functional groups, better model performance is gained when storms are included (*all\_no\_TS\_1*) and the seasonality of the dominant functional group, namely the biomixers, is included (*all\_mix\_TS\_1*). However, model performance decreases when the seasonality of all functional groups is considered (*all\_all\_TS\_1*). The decrease in the model performance due to the inclusion of seasonality is also seen in other experiments which consider only one functional group, while an inclusion of storms only slightly enhances or does not affect the performance of these experiments. On the other hand, an increase in the erosion rate by a factor of 10 improves the performance of the simulations which considers only abiotic drivers (*abio\_x*) and those which include only one functional group (*gra\_x*, *acc\_x*, and *sta\_x*), although their performance is still worse than the experiments with combined effect of all functional groups (*all\_x*).



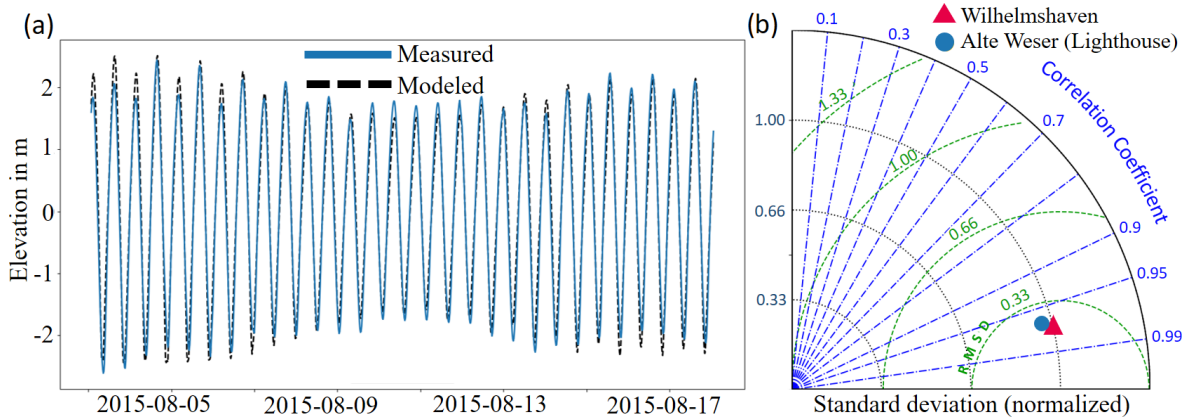


**Figure 3.** (a) Modeled and measured water elevation at the tide gauge station in Wilhelmshaven. (b) Comparison between model results and measurement at the gauge stations in Wilhelmshaven and the Alte Weser Lighthouse in a Taylor diagram.

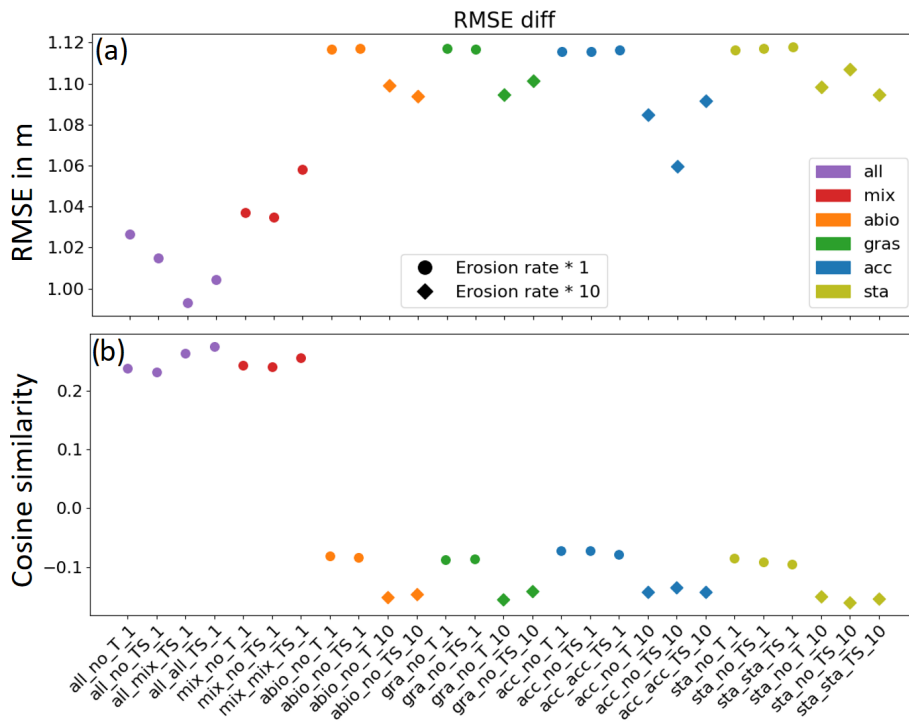


**Figure 4.** Performance of all simulations in terms of (a) RMSE between the modeled and measured water depth change over the entire bay and (b) cosine similarity in the main channels. The values 1, -1, and 0 indicate positive, negative, and no correlation between modeled and measured depth change, respectively. Diamond markers indicate the simulations in which erosion rates were increased by a factor of 10. From left to right, for each experiment with an individual functional group, the model complexity is increased from a normal run without storms and a run including storms to a run including the seasonality of the benthos effect (Table 3).

The cosine similarity between the modeled and measured morphological change provides a further evaluation of the model performance in capturing the change in the main topographic units. It is a measure of similarity between two non-zero vectors which can be derived from the Euclidean dot product. In our evaluation, the cosine similarity is calculated for the main tidal channels (Stenckentief, Vareler Fahrwasser, and Ahne; see Fig. 1). Results (Fig. 4b) show

that in the experiments with all benthos (all\_x) and with the inclusion of only biomix (mix\_x), a positive correlation is found, suggesting that the modeled change is consistent with the measured change. On the contrary, a negative correlation is found in all other experiments, suggesting that an opposite pattern is produced in the model results compared to the measurement. It is worth noting that an increase in the ero-

sion rate by a factor of 10 further strengthens the negative correlation in these experiments.

#### 4.3 Morphological development

The spatial difference in the model results among the experiments and comparison with the measurement is shown in Fig. 5. Measured data indicate net deposition (up to 0.8 m) inside the main tidal channels accompanied by net erosion (up to 1.2 m) at adjacent flats from 2001 to 2009 (Figs. 5b and 6). Compared to a dominant deposition pattern in the channels, the tidal flats exhibit both erosion and deposition in large parts, including various bar-like structures mostly within the range of  $\pm 0.2$  m. However, these structures are likely attributed to artifacts caused by measurement uncertainties and data processing which partly explain the discrepancy in the average depth of tidal flats between measurement and model simulations (Fig. 5). Therefore, we mainly focus on those apparent deposition and erosion patterns in the channels and adjacent flats that exceed the measurement uncertainties. As indicated in the cosine similarity analysis, only the experiments with all benthos (all\_x) and with inclusion of only biomixers (bio\_x) are able to reproduce the extensive deposition pattern in the tidal channels (Figs. 5b and 6), while other experiments including those reference runs which consider only abiotic drivers show the dominance of erosion in the main channels (Figs. 5c and d and 6). The reference run based on the original formulation of erosion rate (Pinto et al., 2012) produces morphological change within the range of  $\pm 0.1$  m (Fig. 5c), which is much smaller than the measured values (Fig. 5a). Only following an increase in the erosion rate by a factor of 10 is the reference run able to produce morphological changes that are at the same order of magnitude as the measurement (Fig. 5d).

There is a net sediment input to Jade Bay from 2001 to 2009 ( $\sim 0.7 \times 10^7 \text{ m}^3$ ), which is indicated by the measurement and captured by model experiments to various extent (Fig. 5). Increased sediment input into Jade Bay was also reported by Benninghoff and Winter (2019). However, most experiments overestimate the volumetric import compared to the measurement, especially on the tidal flats, and the magnitude varies among the experiments (see the Supplement), with largest values in the runs which include the combined effect of all benthos measurement data indicating that the net gain of sediment in the main channel exceeds the net import through the inlet of the bay and suggesting that the sediment accumulated in the channel originates not only from sources external to the bay but also from internal sources, e.g., erosion at adjacent flats. Simulation results suggest that sands accumulated in the channels mainly come from internal sources, while mud may originate from both internal and remote sources outside the bay (Fig. S4). Despite an overestimation of net sediment import to the bay, the model experiments with all benthos included (all\_mix\_TS\_1) produce less deposition in the main channel compared to the measure-

ment (Fig. 6). Instead, much of the imported sediment is deposited over an extensive part of the tidal flats in these runs, as exemplified in Fig. 5a. The reference experiments which include only abiotic drivers (abio\_x) indicate little or no net sediment accumulation in the channel, despite net sediment import through the inlet. In these runs, imported and eroded sediments from the main channel are mostly deposited along the edges of the channels on the flats (Fig. 5c and d).

#### 4.4 Change in sediment composition

There were remarkable changes in sediment composition in Jade Bay from 1996 to 2009, according to Ritzmann and Baumberg (2013). A comparison between the observed change and model results indicates that the changes are largely reproduced in the experiments, but no experiment alone captures all observed changes (Fig. 7). The best performance is shown in the experiments which include all benthos (all\_x). Most of the large-scale changes in sediment composition (indicated by ellipses with roman number I–V) are satisfactorily reproduced in all\_mix\_TS\_1, except for the area in the northwestern part of the bay (I) where an opposite result is shown in the experiment (Fig. 7a, b, and e). On the contrary, experiments which include only abiotic drivers are able to capture the observed change in this area (Fig. 7d and e) but with a worse performance in other areas. The experiment which includes only abiotic drivers and is based on the original formulation of erosion rate (abio\_no\_TS\_1) produces only an increase in the mud content but fails to capture the loss of mud (Fig. 7c and e). Figure 7a illustrates changes in the flat type according to changes in mud content. Since the original mud content change data were not available, the flat-type change instead of the mud content change was compared in this study, which restricts the comparison to a qualitative manner.

#### 4.5 Impact of benthos

To further figure out how the four functional groups of benthos contribute to changes in morphology and sediment composition, we compared the results of the model experiments, which include the impact of individual functional groups, with the reference experiments, which include only abiotic drivers. Since each group of experiments consists of several runs with different levels of complexity (Table 3), we chose the run from each group with the smallest RMSE and same hydrodynamic conditions for comparison, namely abio\_no\_TS\_10, mix\_no\_TS\_1, acc\_no\_TS\_10, gra\_no\_TS\_10, and sta\_no\_TS\_10.

##### 4.5.1 Biomixers

The difference in the depth change between the runs with benthos and the reference run abio\_no\_TS\_10 shows that the largest difference in the morphological change is caused by

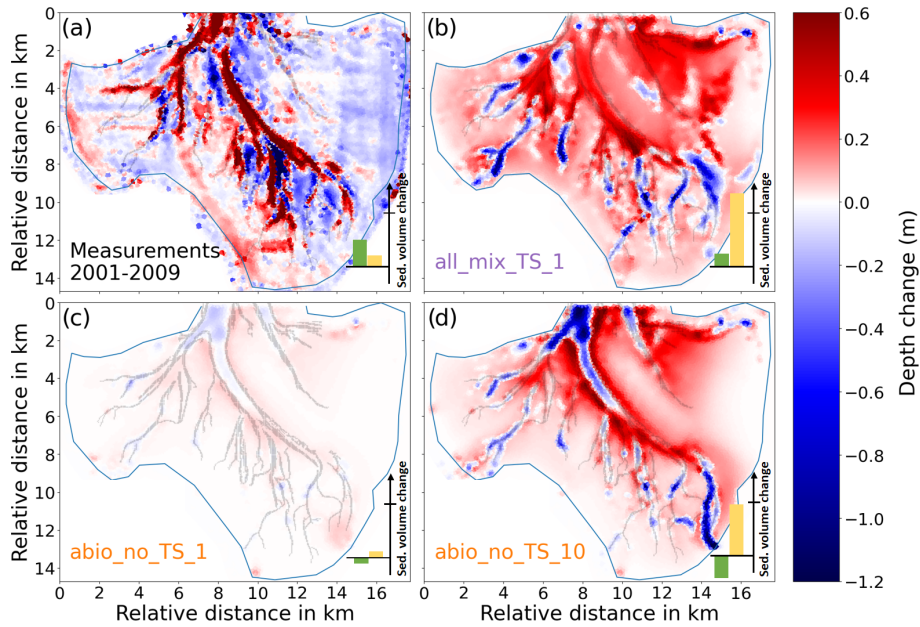


**Figure 5.** Comparison of the morphological change from 2001 to 2009 between the model experiments and the measurement. (a) Results of all\_mix\_TS\_1. (b) Measurement. (c) Results of abio\_no\_TS\_1. (d) Results of abio\_no\_TS\_10. Positive and negative values are for deposition and erosion, respectively. The bars in the lower-right corner represent the total sediment volume change in the main channel (green bar) and the basin excluding the channel (yellow bar). Negative/positive values indicate erosion/deposition. The line across the y axis indicates  $10^7 \text{ m}^3$ . In the measured data, only the grid cells for which the morphological change exceeds the measurement uncertainty (standard deviation of difference between the 2001 and 2009 field data) were included in the sediment budget analysis.

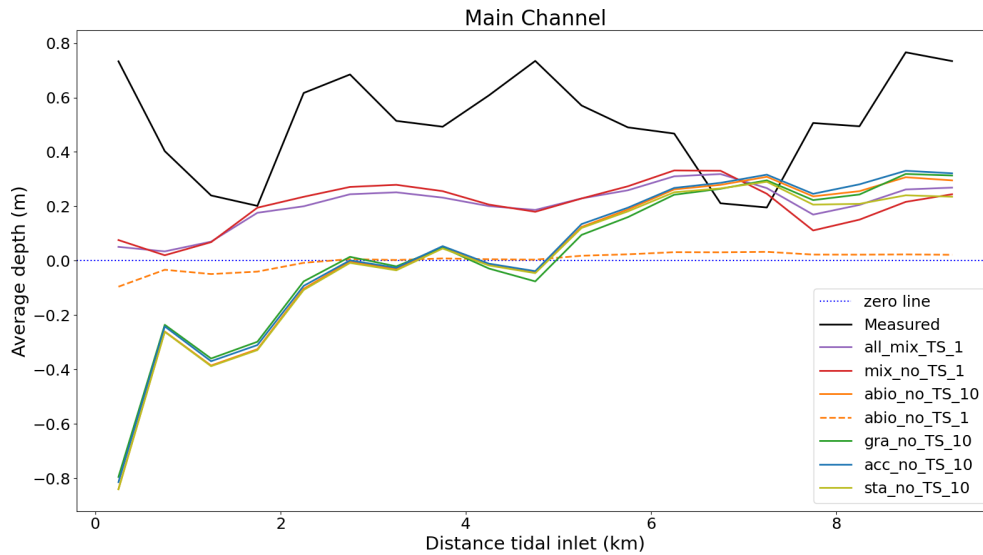


**Figure 6.** Average depth change in the main channel calculated from the measured data and seven representative model experiments between 2001 and 2009. The point at 0 km on the x axis marks the position of the inlet directed into the basin.

biomixers (Fig. 8a), followed by accumulators, seagrass, and stabilizers (Fig. 8b–d). In particular, the extensive accumulation of sediment in the main channel, which is shown in the measurement (Fig. 5a), is associated with the impact of biomixers. The impact of biomixers also causes deposition over a large part of the shallow tidal flats, as well as ero-

sion at the flats adjacent to the tidal channels. The joint effect leads to a smoothing of the depth gradients between the channels and adjacent tidal flats. Morphological changes caused by biomixers are in the range of  $\pm 1 \text{ m}$  compared to the reference run. It is worth noting that biomixers account for not only the enhanced deposition in the main channel but also the

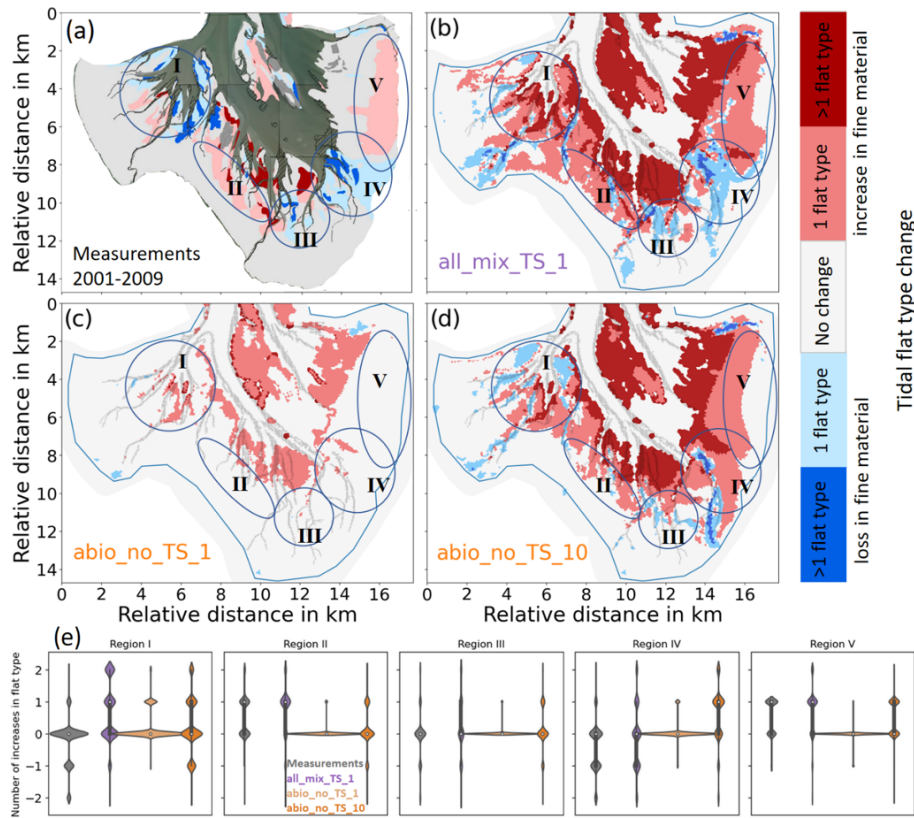


**Figure 7.** Comparison of change in sediment composition between 2001 and 2009 between model results and observation. **(a)** Result of `all_mix_TS_1`. **(b)** Observation. **(c)** Result of `abio_no_TS_1`. **(d)** Result of `abio_no_TS_10`. Pale red and pale blue show the areas where the amount of fine sediment increased or decreased, respectively, with a change by one tidal flat type (according to Fig. 1b). Red and blue show areas with changes by two or more tidal flat types. Areas featuring large-scale changes are marked by ellipses. Panel **(a)** shows a modified version of a plot from Ritzmann and Baumberg (2013) and was kindly provided by the NLWKN (Niedersächsischer Landesbetrieb für Wasserwirtschaft, Küsten- und Naturschutz). The dark gray area in panel **(a)** marks the area where Ritzmann and Baumberg (2013) could not obtain data due to permanent inundation. The roman numerals indicate areas to compare the measurements with the simulations. Panel **(e)** shows the violin plot of the five denoted regions in panels **(a)** to **(d)** for each of the scenarios. The width of the violin plot shows the probability distribution, and the white dot indicates the median.

decrease in the mud content in the southern and southeastern parts (III and IV) of the bay (Fig. 9a and e). These changes are consistent with the field data.

#### 4.5.2 Accumulators

The presence of accumulators causes an overall enhanced deposition over a vast part of the tidal flats, with local values up to 0.5 m when compared to the reference run (Fig. 8b). The average deposition over at the tidal flats is highest compared to other simulations (Fig. S6b). Accumulators do not seem to directly impact the morphological change (I) the tidal channels; however, model results show that they can lead to a significant increase in the mud content in a vast part of the bay including the channels (Fig. 9b and e). In particular, the observed increase in the mud content in the southwestern part (II) of the bay is attributed to the impact of accumulators according to the model result.

#### 4.5.3 Seagrass

Our simulation results suggest that the impact of seagrass on morphological change in Jade Bay is smaller than that of biominerers and accumulators when looking at the overall depth change (dark red and blue bars in Fig. 8). However, local changes might be higher compared to the accumulator scenarios (Fig. 8b and c). Furthermore, instead of tidal flats, channels and areas adjacent to seagrass meadows are particularly under high impact. In the eastern part of the bay where seagrass is present, a slight deposition in the range of 20 cm occurs at the edge and at the outer parts of the seagrass meadows (Fig. 8c). Meanwhile, mud content decreases in the same area, suggesting a winnowing process there (Fig. 9c and e).

Interestingly, seagrass meadows not only affect sediment transport and morphodynamics in the direct vicinity around their habitats but also cause far-reaching changes over the bay, including the channels and other flats that are free of

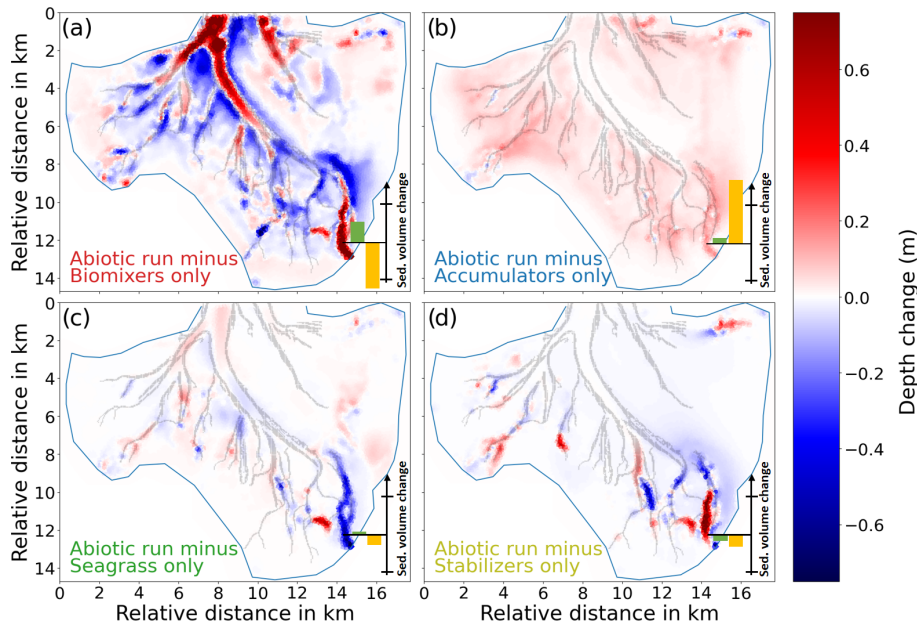


**Figure 8.** Difference in the depth change between the reference run `abio_no_TS_10` and (a) `mix_no_TS_1`, (b) `acc_no_TS_10`, (c) `gra_no_TS_10`, and (d) `sta_no_TS_10`. Positive and negative values indicate increased deposition and erosion, respectively, in the runs with benthos compared to the reference run. The bars in the lower-right corner represent the total sediment volume change in the main channel (green bar) and the basin excluding the channel (yellow bar). Negative/positive values indicate erosion/deposition. The lines across the y axis indicate  $\pm 3 \times 10^6 \text{ m}^3$ .

seagrass (Figs. 8c and 9c). This effect is through a feedback of seagrass meadows to larger-scale hydrodynamics. The ratio in the transported volume between the flooding and the ebbing phase calculated from the simulation results indicates that the majority of water enters Jade Bay through its main channels during the flooding phase and leaves it over the tidal flats during the ebbing phase (Fig. S5a). The spillway on the tidal flats in the eastern part of the bay (V), where seagrass meadows are located, experiences larger flow friction due to the presence of seagrass (Fig. S5b). As a consequence, more water is transported through the main channel, eroding more fine-grained sediments compared to the abiotic scenario (Fig. S5c). Thus, the increased loss of fine-grained sediment in the main channel (Fig. 9c and e) correlates significantly with the changed water flux in the main channel (Fig. S5c).

#### 4.5.4 Stabilizers

The impact of stabilizers on the morphological changes in Jade Bay is comparable to that of seagrass in magnitude. The resultant morphological change is mostly local within the habitats of stabilizers and featured by both erosion and deposition (Fig. 8d). Sediment stabilization and consolidation in the areas where stabilizers exist lead to reduction in the sediment sources for the distal ends of small channels, preventing the mobilization of sediments in these parts. Compared to the abiotic run, the sediment budget in the tidal flat is negative

(Fig. 8d). This is attributed to the stabilization of tidal flats outside of Jade Bay, leading to less erosion there and thus less sediment transport from outside into Jade Bay. The impact of stabilizers on sediment composition is more prominent compared to the morphological change. In the subtidal area, a significant decrease in the mud content is seen in the simulation result compared to the reference experiment (Fig. 9d and e) as a consequence of reduced mud input from stabilized areas that are predominantly on the distant tidal flats.

## 5 Discussion

### 5.1 Model hindcast and implication

The model performance, both in terms of morphology and sediment distribution, is improved when biota are included in the simulation. In particular, the extensive deposition in the main channels is reproduced only by the experiments with either combined effect of all benthos (`all_x`) or with biomixers (`mix_x`), while other experiments produce an opposite pattern.

Our simulation results show that, among all four functional groups considered in the modeling, biomixers are most impactful on morphological change in Jade Bay, followed by accumulators, seagrass, and stabilizers. The morphological change in the bay over the 8.5-year period (2001–2009) features distinct deposition inside the main channels and erosion at their adjacent flats (Fig. 5a). This feature and the

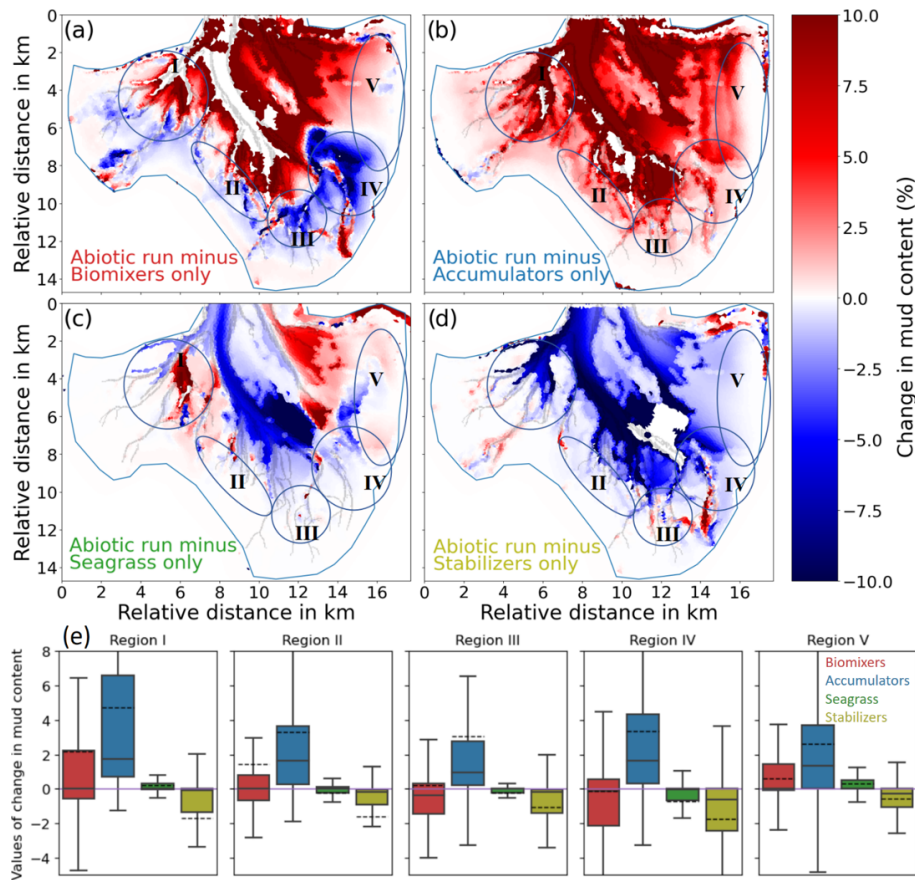


**Figure 9.** Difference in the mud content (%) between the reference run\_abio\_no\_TS\_10 and (a) mix\_no\_TS\_1, (b) acc\_no\_TS\_10, (c) gra\_no\_TS\_10, and (d) sta\_no\_TS\_10. Panel (e) shows the box plot diagram of the five denoted regions in panels (a) to (d) for each of the scenarios. The zero line is indicated in purple. The median (solid black line) and the mean (dashed black line) are shown in the box plot.

amount of deposited sediment could be reproduced by modeling only when the impact of benthos, especially biomixers, is included.

The impact of biomixers on sediment is mainly destabilization (Arlinghaus et al., 2021) but can, under certain circumstances, exert stabilization as well (Cozzoli et al., 2019). This depends on the metabolic rate, bottom shear stress, and sediment composition. Muddy sediment particles in general have a higher organic matter content and therefore higher nutritional value than sands and are hence more intensively reworked and bioturbated by benthic fauna (Arlinghaus et al., 2021). In sandy sediments, benthos-produced mucus exerts a stabilization impact which often exceeds the destabilization impact because of less bioturbation (Orvain, 2002; Le Hir et al., 2007). For this reason, the channel deposition can be explained by two factors related to macrobenthos. First, the critical shear stress for erosion is increased by the presence of biomixers ( $p_d > 1$  in Eq. 1; Fig. S3) in the sandy channels, leading to enhanced resistance to erosion. Second, enhanced erosion on the tidal flats by biomixers ( $p_d < 1$ ,  $g_d > 1$ ) mobilizes sands which are partly deposited in the channel. Mud

can hardly accumulate in the channel due to a low sinking velocity and low threshold for resuspension (before consolidation). The majority of the accumulated sands in the channels comes from the eroded tidal flats. The redistribution of sediments from the tidal flats, which become increasingly deeper, into the channels, which become shallower, represents a typical basin development pattern under the impact of biotic destabilization as demonstrated by Arlinghaus et al. (2022). This is the case for Jade Bay, where a shift in the functional groups took place between the 1970s and 2000s with biomixers increasing from  $\sim 20\%$  to almost  $70\%$  in the field surveys (Schückel and Kröncke, 2013). Furthermore, the channel incision and sediment deposition at its edges in the model experiment, which only considers abiotic drivers, compare well with the abiotic scenario presented in Arlinghaus et al. (2022), who asserted that deep and narrow channels develop with shallow tidal flats. The effect of unrealistically strong channel incision is known in morphodynamic modeling, although this problem is often overlooked (Baar et al., 2019). One practical solution that is often adopted in applications is an increase in the bed slope diffusion, e.g., by

up to a factor of 100 (Van der Wegen and Roelvink, 2012; Schuurman et al., 2013; Braat et al., 2017). However, this solution does not represent a process-based understanding. An alternative solution is provided in our modeling study, which proposes to include the impact of bioturbation instead of tuning the bed slope diffusion.

Compared to the remarkable impact of bioturbators which leads to deposition in the channels and erosion in the flats and therefore a general widening of channels, other functional groups have less influence on the morphological change in the main channels according to our simulation results. Accumulators mainly enhance sediment deposition on the tidal flats. Seagrass meadows can modify the flows not only within or adjacent to their habitats but also at a large scale, covering a vast part of the bay, which results in alternating erosion and deposition patterns in the main channel. The impact of stabilizers on the morphological change in Jade Bay is small compared to bioturbators and accumulators. This is attributed to their location. The shallow tidal flats in the south and west of Jade Bay which are inhabited by stabilizers are subject to relatively weak tidal currents and low SSC. The different impacts of the mentioned functional groups in Jade Bay are depicted in a simplified form in Fig. 10, where sediment redistribution (e.g., from tidal flats to channels) and vertical erosion/deposition patterns are distinguished. Our results suggest benthos as a critical driver determining sediment stability and morphological development of tidal embayments and basins, supporting an earlier study by Backer et al. (2010). A reference simulation, which considers only abiotic drivers and adopts formulation of erosion rates from laboratory experiments in which benthos is excluded, heavily underestimates the morphological change. An increase in the erosion rate by a factor of 10 allows the reference simulation to produce morphological changes that are at the same order of magnitude with the measurement but still fails to capture the spatial pattern. This indicates that existing formulations for sediment resuspension rate that do not take into account the fact that benthos impact may be of limited use for application to real coastal systems that are inhabited by benthos.

As demonstrated in the model results, the major effect of benthos is sediment mobilization and redistribution, which was also found in Borsje et al. (2008) and Lumborg et al. (2006). Especially the import of mud into the bay is increased under the impacts of benthos, which is in line with other modeling results summarized in Arlinghaus et al. (2021). Our results show that accumulators have the strongest impact on changes in sediment composition, followed by bioturbators, seagrass, and stabilizers. The impact of accumulators is mostly local, but this functional group is present over a vast part of the bay and thus jointly leads to a large-scale impact. By contrast, the impact of bioturbators extends beyond their habitats. Locally, sediment can be either stabilized or destabilized, depending on the abundance of bioturbators and other factors elucidated previously. Non-locally, the enhanced erosion in large parts of the tidal flats by bioturbators increases

the overall concentration of suspended sediment, especially on the flats outside Jade Bay, which provides a sediment source for the bay. The impact of seagrass is prominent in close vicinity to the meadows but not so much within the meadow itself. One explanation is that the effect of organic sediment accumulation due to primary and detritus production and root and rhizome formation, which are main sources for sediment production (Gacia et al., 2003), was not considered in this study. The found changes close to the meadows are in line with measurements indicating differences in bed level elevation between vegetated and nonvegetated areas in the range of  $3 \text{ cm yr}^{-1}$  (Potouroglou et al., 2017). The impact of seagrass meadows also reaches beyond their habitats by altering the large-scale hydrodynamics and the ratio of the inflow to the outflow in the tidal channels and on the flats. The increased loss of mud content in the tidal channels in the stabilizers experiments compared to the reference run can be explained by the reduced supply of mud from the tidal flats which are inhabited by stabilizers. However, since the mud content is small in the hydrodynamically active areas, the absolute change in the mud content induced by stabilizers is minor.

The changes in sediment composition are reproduced more satisfactorily in four areas with the inclusion of benthos effects, namely the southern (III), the southeastern (IV), the eastern (V), and the southwestern (II) parts of the bay (Fig. 7). The loss of mud due to erosion in the southern (III) and the southeastern (IV) parts is mostly attributed to the impact of bioturbators, which has a strong destabilization effect there. The eastern (V) part accumulates much more fine sediment compared to the reference run, which is attributed to the impact of seagrass and accumulators (Fig. 9). This impact might even be enhanced in reality due to the organic sediment accumulation explained above. The increase in the mud content on the shallow tidal flats in the southwestern part is mainly due to the presence of accumulators. At one site in the western part, the reference simulation yields better results with a loss of mud, which is not captured by experiments with benthos.

Overall, the increase in the mud content is overestimated in all model experiments when compared to the field data. One possible explanation is that mixing between sediment layers, which gets enhanced by bioturbators, was not implemented in the model and thus all freshly deposited mud remains on the seabed surface before being eroded at a later stage or buried by further new deposits, while mixing in the sediment column in a natural system would mix freshly deposited mud and organic matter with other coarser particles and lead to homogenization of sediment grain size in the upper 10–30 cm, as pointed out by previous studies (Knaapen et al., 2003; Paarlberg et al., 2005; Arlinghaus et al., 2022).

It should be noted that the dominant impact of bioturbators and accumulators is related to their widespread abundance and high biomass in Jade Bay. In other environments, different functional groups may dominate. For instance, some

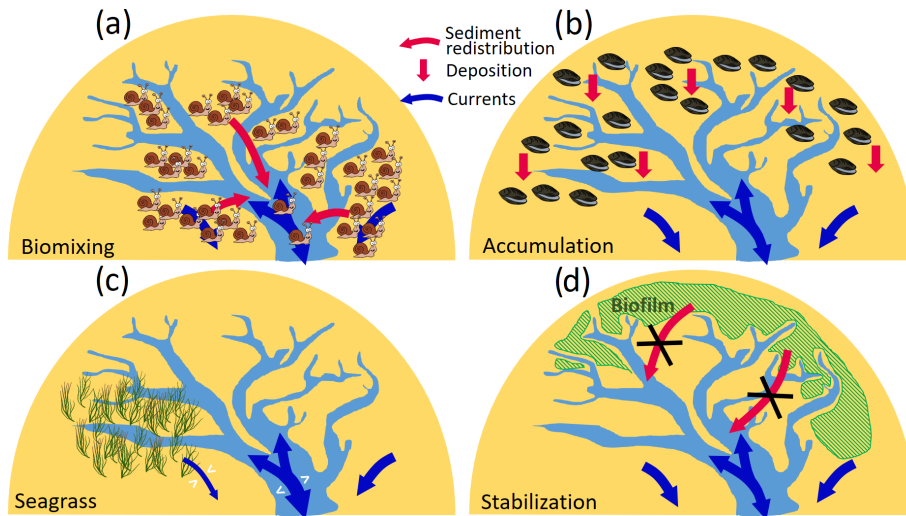


**Figure 10.** Conceptual sketch of different effects of the four functional groups on sedimentation and hydrodynamics in tidal embayments. (a) Destabilization in tidal flats caused by biomixers. (b) Accumulation caused by filter/suspension feeders. (c) Modification of flooding/ebb-ing flows by seagrass meadows. (d) Sediment stabilization by MPB and reduced input to channels.

modeling studies show a significant impact of seagrass on the morphodynamics of tidal basins (Mohr, 2022), barrier islands (Reeves et al., 2020), and estuaries (Walter et al., 2020). Seagrass impact may further complicate when their effect interacts with other plants such as salt marshes (Carr et al., 2018). Unfortunately, a quantitative comparison of the impact normalized to biomass between the different functional groups cannot be made in this study due to a lack of biomass data for seagrass and stabilizers in the study area, which points out a need for future studies.

## 5.2 Societal relevance

Similar to many other coastal bays/embayments worldwide, Jade Bay serves important socioeconomic functions for tourism and logistics, and on the other hand, Jade Bay provides important refuge for a variety of marine life-forms. It is of critical importance to sustain the ecological functions of coastal bays such as Jade Bay under the increasing pressure of human use and climate change. Our results indicate that benthos can significantly modify morphological change and sediment composition in tidal embayments and can play a key role in the natural resilience of coastal systems against human and climate stressors. However, we also revealed that the impact on morphological development varies among different functional groups. Biomixers tend to smooth the bathymetric gradients between channels and flats, while seagrass and accumulators may counteract this to various extents. A combined effect of all functional groups leads to the increased import of sediment, especially mud, to the bay. Our results support the hypothesis by Haas et al. (2018), who proposed that an abundance of mud and eco-engineering species often culminates in continuous embayment filling with fine

sediment and the growth of intertidal and supratidal areas, eventually leading to closure of the embayment. However, on the other hand, there is growing concern about whether coastal systems such as the Wadden Sea and including Jade Bay can keep pace with the foreseeable sea level rise for the upcoming decades (Plater and Kirby, 2011). Our results show that the morphological development of Jade Bay is able to sustain the impact of sea level rise, at least for the period 2001–2009, because of a net sediment import caused by a joint effect of abiotic and biotic drivers. But it is unclear how the drivers would change in future, especially with respect to how the different functional groups of benthos would react to human and climate stressors. For instance, chlorine inputs are expected to increase in Jade Bay due to the construction of liquefied natural gas (LNG) terminals, which will likely have an impact on the population, abundance, and distribution of the different functional groups. This may result in a loss of sensitive species and functional groups, as pointed out by studies in other regions (Chang, 1989; Wang et al., 2022). Extreme weather events, such as heatwaves, also have a significant impact on benthos (Serrano et al., 2021). The intensity and frequency of extreme events are likely to increase in the future due to climate change, but the consequent change in benthos remains largely unknown. To this end, explanatory and eventually predictive numerical models are imperative for exploring feasible nature-based solutions for sustaining both socioeconomic and ecological functions of coastal regions.

## 5.3 Model limitations and future research needs

Earth system modeling and regional modeling inevitably comprise uncertainties which originate from various sources



including boundary conditions, numerical solvers, and the parameterization of processes. This is especially true in the modeling of coastal systems in which physical and biological factors may be of comparable importance in guiding the system evolution. Model refinement and/or inclusion of additional processes do not necessarily increase model accuracy, since the uncertainties in parameterization of less-known processes (e.g., growth/decline in benthos and interactions between different species/functional groups) may exceed the gain in accuracy (Skinner et al., 2018; Pianosi et al., 2016). An earlier study found that it remains a challenge to get physically correct results for both sediment transport and morphodynamics simultaneously (Baar et al., 2019). Therefore, the development of hydro-eco-morphodynamic models will always be limited to a certain tradeoff between complexity and accuracy. This is confirmed in our study, which indicates that an increase in model complexity by considering the benthos impact first increases model performance in approximating observed change but that model performance decreases when a higher complexity, i.e., seasonal change in benthos, is added by a simple parameterization. This points out a need for an accurate mapping of benthos, including the temporal changes in the field which can serve input for the modeling and/or process-based understanding and formulation of the temporal change in benthos for modeling.

## 6 Conclusions

We have presented an effort towards large-scale explanatory hydro-eco-morphodynamic modeling to explain changes in both the morphology and sediment composition observed in a real coastal system, thereby disentangling the impacts of biotic and abiotic drivers. The following conclusions are drawn from the study.

Benthos significantly reworks sediment, thereby mediating large-scale and long-term change in the coastal morphology and seabed sediment properties well beyond their habitats. Compared to the scenarios which include only abiotic drivers, simulations with benthos included produced significantly improved results that are closer to observation and are able to explain some unique features in the historical change in the morphology and sediment composition in Jade Bay. The most impactful functional group regarding morphological change in Jade Bay is biomixers. The impact of biomixers leads to prominent sediment accumulation in the main channels. Accumulators mainly enhance sediment deposition on the tidal flats. Seagrass meadows modify the flows not only within or adjacent to the sites where they are located but also at a much larger scale beyond their habitats, resulting in alternating erosion and deposition patterns in the main channels. Stabilizers locally prevent the mobilization of sediments on the distant tidal flats. Regarding the change in the sediment composition in Jade Bay, accumulators have the strongest impact. The impact of accumulators is mostly local, but this

functional group is present over a vast part of the bay and thus jointly leads to a large-scale impact. By contrast, the impact of biomixers, seagrass, and stabilizers on sediment composition extends beyond their habitats. A combined effect of all functional groups leads to the increased import of sediment, especially mud, to the bay. Also, results indicate that the impacts of functional groups can both counteract and enhance each other. An increased SSC level by biomixers, for instance, enhances the impact of other functional groups. On the other hand, biomixing-induced sediment erosion on the tidal flats is partly offset by the bio-deposition of accumulators.

Our results further show that increasing model complexity does not necessarily lead to better model performance, especially when biotic drivers such as benthos are included. Including storm surges, which are precisely described by observational data, improves model performance. By contrast, adding seasonality to the benthos impact through an oversimplified parameterization decreases the general model performance. The reason is attributed to a lack of observational data which can support a more accurate formulation of temporal changes in benthos behaviors. Therefore, the complexity of hydro-eco-morphodynamic models should be balanced at a certain level on which a tradeoff between complexity and accuracy can be obtained.

Coastal systems such as Jade Bay have important socio-economic and ecological functions worldwide. Therefore, the development of advanced numerical models which are able to explain and predict the states of coastal morphology and sediment properties and to develop measures for protection is of vital importance. To achieve this step, further effort in numerical modeling should explicitly include biotic drivers such as benthos and deepen the understanding of the interactions between different functional groups and between biota and abiotic drivers. In this sense, not only dedicated field measurements and lab experiments but also large-scale and long-term monitoring are indispensable.

**Data availability.** Publicly available datasets were analyzed in this study. Morphological data of the German Bight can be found at <https://doi.org/10.48437/02.2020.K2.7000.0002> (Sievers et al., 2020). Sea level data at the tide gauge station of Wilhelmshaven can be found at <https://emodnet.ec.europa.eu/geoviewer/> (WSV, 2023; Calewaert et al., 2016).

**Supplement.** The supplement related to this article is available online at: <https://doi.org/10.5194/esurf-12-537-2024-supplement>.

**Author contributions.** PA designed the study and performed numerical simulations. WZ designed and supervised the study. PA and WZ wrote the paper. IK provided the infauna dataset. All four authors were involved in revising the paper.

**Competing interests.** The contact author has declared that none of the authors has any competing interests.

**Disclaimer.** Publisher's note: Copernicus Publications remains neutral with regard to jurisdictional claims made in the text, published maps, institutional affiliations, or any other geographical representation in this paper. While Copernicus Publications makes every effort to include appropriate place names, the final responsibility lies with the authors.

**Acknowledgements.** This study is a contribution to the I<sup>2</sup>B project “Unravelling the linkages between benthic biological functioning, biogeochemistry and coastal morphodynamics – from big data to mechanistic modelling” funded by Helmholtz-Zentrum Hereon. It is also supported by the Helmholtz PoF programme “The Changing Earth – Sustaining our Future” on its Topic 4: Coastal zones at a time of global change.

The benthic infauna dataset from 2009 was kindly provided by Senckenberg am Meer. The sediment map was provided by the NLWKN (Niedersächsischer Landesbetrieb für Wasserwirtschaft, Küsten- und Naturschutz).

**Financial support.** The article processing charges for this open-access publication were covered by the Helmholtz-Zentrum Hereon.

**Review statement.** This paper was edited by Claire Masteller and Andreas Lang and reviewed by Matthew Hiatt and two anonymous referees.

## References

- Adolph, W.: Praxistest Monitoring Küste 2008: Seegraskartierung: Gesamtbestandserfassung der eulitoralischen Seegrasbestände im Niedersächsischen Wattenmeer und Bewertung nach EU-Wasserrahmenrichtlinie, NLWKN Küstengewässer und Ästuar, 2, 1–62, [https://www.nlwkn.niedersachsen.de/download/54316/Seegraskartierung\\_Gesamtbestandserfassung\\_2008\\_.....Band\\_2\\_2010.pdf](https://www.nlwkn.niedersachsen.de/download/54316/Seegraskartierung_Gesamtbestandserfassung_2008_.....Band_2_2010.pdf) (last access: 19 April 2024), 2010.
- Andersen, T. and Pejrup, M.: Biological influences on sediment behavior and transport, in: Treatise on estuarine and coastal science, vol. 2, edited by: Wolanski, E. and McLusky, D. S., Academic Press, Waltham, 289–309, <https://doi.org/10.1016/B978-0-12-374711-2.00217-5>, 2011.
- Arlinghaus, P., Zhang, W., Wrede, A., Schrum, C., and Neumann, A.: Impact of benthos on morphodynamics from a modeling perspective, *Earth-Sci. Rev.*, 221, 103803, <https://doi.org/10.1016/j.earscirev.2021.103803>, 2021.
- Arlinghaus, P., Zhang, W., and Schrum, C.: Small-scale benthic faunal activities may lead to large-scale morphological change- A model based assessment, *Front. Mar. Sci.*, 9, 1011760, <https://doi.org/10.3389/fmars.2022.1011760>, 2022.
- Baar, A. W., Boechat Albernaz, M., van Dijk, W. M., and Klein-hans, M.: Critical dependence of morphodynamic models of fluvial and tidal systems on empirical downslope sediment transport, *Nat. Commun.*, 10, 4903, <https://doi.org/10.1038/s41467-019-12753-x>, 2019.
- Backer, A., Van Colen, C., Vincx, M., and Degraer, S.: The role of biophysical interactions within the IJzermondig tidal flat sediment dynamics, *Cont. Shelf Res.*, 30, 1166–1179, <https://doi.org/10.1016/j.csr.2010.03.006>, 2010.
- Becker, M.: Suspended Sediment Transport and Fluid Mud Dynamics in Tidal Estuaries, PhD thesis, University of Bremen, <http://nbn-resolving.de/urn:nbn:de:gbv:46-00102481-14> (last access: 19 April 2024), 2011.
- Benninghoff, M. and Winter C.: Recent morphologic evolution of the German Wadden Sea, *Sci. Rep.-UK*, 9, 9293, <https://doi.org/10.1038/s41598-019-45683-1>, 2019.
- Beukema, J.: Seasonal changes in the biomass of the macro-benthos of a tidal flat area in the Dutch wadden Sea, *Neth. J. Sea Res.*, 8, 94–107, [https://doi.org/10.1016/0077-7579\(74\)90028-3](https://doi.org/10.1016/0077-7579(74)90028-3), 1974.
- Beukema, J. J. and Dekker, R.: Half a century of monitoring macrobenthic animals on tidal flats in the Dutch wadden Sea, *Mar. Ecol. Prog. Ser.*, 8, 1–18, <https://doi.org/10.3354/meps13555>, 2020.
- Borsje, B. W., de Vries, M., Hulscher, S., and de Boer, G.: Modeling large-scale cohesive sediment transport affected by small-scale biological activity, *Estuar. Coast. Shelf S.*, 78, 468–480, <https://doi.org/10.1016/j.ecss.2008.01.009>, 2008.
- Braat, L., van Kessel, T., Leuven, J. R. F. W., and Klein-hans, M. G.: Effects of mud supply on large-scale estuary morphology and development over centuries to millennia, *Earth Surf. Dynam.*, 5, 617–652, <https://doi.org/10.5194/esurf-5-617-2017>, 2017.
- Brückner, M., Schwarz, C., Coco, G., Baar, A., Boechat Albernaz, M., and Klein-hans, M.: Benthic species as mud patrol – modelled effects of bioturbators and biofilms on large-scale estuarine mud and morphology, *Earth Surf. Proc. Land.*, 46, 1128–1144, <https://doi.org/10.1002/esp.5080>, 2021.
- Cai, X.: Impact of Submerged Aquatic Vegetation on Water Quality in Cache Slough Complex, Sacramento-San Joaquin Delta: a Numerical Modeling Study. Dissertations, Theses, and Masters Projects, Paper 1550153628, William & Mary, <https://doi.org/10.25773/v5-8snw-1660>, 2018.
- Calewaert, J. B., Weaver, P., Gunn, V., Goringe, P., and Novellino, A.: The European Marine Data and Observation Network (EMODnet): Your Gateway to European Marine and Coastal Data, Springer, [https://doi.org/10.1007/978-3-319-32107-3\\_4](https://doi.org/10.1007/978-3-319-32107-3_4), 2016.
- Carr, J., Mariotti, G., Fahgerazzi, S., McGlathery, K., and Wiberg, P.: Exploring the Impacts of Seagrass on Coupled Marsh-Tidal Flat Morphodynamics, *Front. Environ. Sci.*, 6, 92, <https://doi.org/10.3389/fenvs.2018.00092>, 2018.
- Chang, V.: An on-site assessment of chlorination impacts on benthic macroinvertebrates, Master thesis, University of Massachusetts Amherst, <https://doi.org/10.7275/20482910>, 1989.
- Chen, X. D., Zhang, C. K., Paterson, D. M., Thompson, C. E., Townend, I. H., Gong, Z., Zhou, Z., and Feng, Q.: Hindered erosion: The biological mediation of noncohesive sediment behavior, *Water Resour. Res.*, 53, 4787–4801, <https://doi.org/10.1002/2016WR020105>, 2017.

- Corenblit, D., Baas, A., Bornette, G., Darrozes, J., Delmotte, S., Francis, R., Gurnell, A., Julien, F., Naiman, R., and Steiger, J.: Feedbacks between geomorphology and biota controlling Earth surface processes and landforms: A review of foundation concepts and current understandings, *Earth-Sci. Rev.*, 106, 307–331, <https://doi.org/10.1016/j.earscirev.2011.03.002>, 2011.
- Cozzoli, F., Gjoni, V., Del Pasqua, M., Hu, Z., Ysebaert, T., Herman, M. J. P., and Bouma, T.: A process based model of cohesive sediment resuspension under bioturbators' influence, *Sci. Total Environ.*, 670, 18–30, <https://doi.org/10.1016/j.scitotenv.2019.03.085>, 2019.
- Daggers, T. D., Herman, P. M., and van der Wal, D.: Seasonal and Spatial Variability in Patchiness of Microphytobenthos on Intertidal Flats From Sentinel-2 Satellite Imagery, *Frontiers in Marine Science*, 7, 392, <https://doi.org/10.3389/fmars.2020.00392>, 2020.
- Desjardins, E., Van De Wiel, M., and Rousseau, Y.: Predicting, explaining and exploring with computer simulations in fluvial geomorphology, *Earth-Sci. Rev.*, 209, 102654, <https://doi.org/10.1016/j.earscirev.2018.06.015>, 2018.
- De Troch, M., Cnudde, C., Vyverman, W., and Vanreusel, A.: Increased production of faecal pellets by the benthic harpacticoid *Paramphiascella fulvofasciata*: Importance of the food source, *Mar. Biol.*, 156, 469–477, <https://doi.org/10.1007/s00227-008-1100-2>, 2008.
- Duong, T., Ranasinghe, R., Walstra, D. J., and Roelvink, D.: Assessing climate change impacts on the stability of small tidal inlet systems: Why and how?, *Earth-Sci. Rev.*, 154, 369–380, <https://doi.org/10.1016/j.earscirev.2015.12.001>, 2016.
- French, J., Payo, A., Murray, A. B., Orford, J., Eliot, M., and Cowell, P.: Appropriate complexity for the prediction of coastal and estuarine geomorphic behaviour at decadal to centennial scales, *Geomorphology*, 256, 3–16, <https://doi.org/10.1016/j.geomorph.2015.10.005>, 2015.
- Gacia, E., Duarte, C. M., Marbà, N., Terrados, J., Kennedy, H., Fortes, M. D., and Tri, N. H.: Sediment deposition and production in SE-Asia seagrass meadows, *Estuar. Coast. Shelf S.*, 56, 909–919, [https://doi.org/10.1016/S0272-7714\(02\)00286-X](https://doi.org/10.1016/S0272-7714(02)00286-X), 2003.
- Galbiati, L., Somma, F., and Zaldivar-Comenges, J. M.: Pilot River Basin Activity Report 15 Phase II: 2005–2006, EUR – Scientific and Technical Research series, 172 pp., <https://doi.org/10.2788/72161>, 2008.
- Glud, R., Gundersen, J., Røy, H., and Jørgensen, B.: Seasonal Dynamics of Benthic O<sub>2</sub> Uptake in a Semienclosed Bay: Importance of Diffusion and Faunal Activity, *Limnol. Oceanogr.*, 48, 1265–1276, <https://doi.org/10.4319/lo.2003.48.3.1265>, 2003.
- Götschenberg, A. and Kahlfeld, A.: The Jade, *Kueste*, 74, 263–274, 2008.
- Graf, G. and Rosenberg, R.: Bioresuspension and biodeposition: a review, *J. Marine Syst.*, 11, 269–278, [https://doi.org/10.1016/S0924-7963\(96\)00126-1](https://doi.org/10.1016/S0924-7963(96)00126-1), 1997.
- Grant, J. and Daborn, G.: The effects of bioturbation on sediment transport on an intertidal mudflat, *Neth. J. Sea Res.*, 32, 63–72, [https://doi.org/10.1016/0077-7579\(94\)90028-0](https://doi.org/10.1016/0077-7579(94)90028-0), 1994.
- Haas, T., Pierik, H., Van der Spek, A. J. F., Cohen, K., van Maanen, B., and Kleinhans, M.: Holocene evolution of tidal systems in The Netherlands: Effects of rivers, coastal boundary conditions, eco-engineering species, inherited relief and human interference, *Earth-Sci. Rev.*, 177, 139–163, <https://doi.org/10.1016/j.earscirev.2017.10.006>, 2018.
- Jone, S. C., Lawton, J. H., and Shachak, M.: *Organisms as Ecosystem Engineers*, Ecosystem Management, Springer, [https://doi.org/10.1007/978-1-4612-4018-1\\_14](https://doi.org/10.1007/978-1-4612-4018-1_14), 1994.
- Kahlfeld, A. and Schüttrumpf, H.: UnTRIM modelling for investigating environmental impacts caused by a new container terminal within the Jade-Weser Estuary, German Bight, in: *Proceedings of the Seventh International Conference on Hydroscience and Engineering*, 18 April 2007 <https://researchdiscovery.drexel.edu/esploro/outputs/991014632386204721> (last access: 19 April 2024), 2006.
- Knaapen, M., Holzhauer, H., Hulscher, S. J. M. H., Baptist, M. J., de Vries, M., and van Ledden, M.: On the modelling of biological effects on morphology in estuaries and seas, in: Sánchez-Arcilla, A. and Bateman, A., RCEM 2003, *Proceedings of the Third IAHR Symposium on River, Coastal and Estuarine Morphodynamics, IHAR*, 773–783, <https://research.utwente.nl/en/publications/on-the-modelling-of-biological-effects-on-morphology-in> (last access: 22 April 2024), 2003.
- Kristensen, E., Penha-Lopes, G., Delefosse, M., Valdemarsen, T., Organo Quintana, C., and Banta, G.: What is bioturbation? Need for a precise definition for fauna in aquatic science, *Mar. Ecol. Prog. Ser.*, 446, 285–302, <https://doi.org/10.3354/meps09506>, 2012.
- Lang, G.: Ein Beitrag zur Tidedynamik der Innenjade und des Jadebusens, *Mitteilungsblatt der Bundesanstalt für Wasserbau*, Nr. 86, Karlsruhe, [https://izw.baw.de/publikationen/mitteilungsblaetter/0/lang\\_jade.pdf](https://izw.baw.de/publikationen/mitteilungsblaetter/0/lang_jade.pdf) (last access: 19 April 2024), 2003.
- Larsen, L., Eppinga, M., Passalacqua, P., Getz, W., Rose, K., and Liang, M.: Appropriate complexity landscape modeling, *Earth-Sci. Rev.*, 160, 111–130, <https://doi.org/10.1016/j.earscirev.2016.06.016>, 2016.
- Le Hir, P., Monbet, Y., and Orvain, F.: Sediment erodability in sediment transport modelling: can we account for biota effects?, *Cont. Shelf Res.*, 27, 1116–1142, <https://doi.org/10.1016/j.csr.2005.11.016>, 2007.
- Levin, L., Boesch, D., Covich, A., Dahm, C., Erséus, C., Ewel, K., Kneib, R., Moldenke, A., Palmer, M., Snelgrove, P., Strayer, D., and Weslawski J.: The function of marine critical transition zones and the importance of sediment biodiversity, *Ecosystems*, 4, 430–451, <https://doi.org/10.1007/s10021-001-0021-4>, 2001.
- Lindqvist, S., Engelbrektsson, J., Eriksson, S. P., and Hulth, S.: Functional classification of bioturbating macrofauna in marine sediments using time-resolved imaging of particle displacement and multivariate analysis, *Biogeosciences Discuss.* [preprint], <https://doi.org/10.5194/bg-2016-411>, 2016.
- Linke, O.: Die Biota des Jadebusenwattes, *Helgol. Wiss. Meer.*, 1, 201–348, <https://doi.org/10.1007/BF02242420>, 1939.
- Luan, J., Zhang, C., Xu, B., Xue, Y., and Ren, Y.: The predictive performances of random forest models with limited sample size and different species traits, *Fish. Res.*, 227, 105534, <https://doi.org/10.1016/j.fishres.2020.105534>, 2020.
- Lumborg, U., Andersen, T., and Pejrup, M.: The effect of *Hydrobia ulvae* and microphytobenthos on cohesive sediment dynamics on an intertidal mudflat described by means of

- numerical modelling, *Estuar. Coast. Shelf S.*, 68, 208–220, <https://doi.org/10.1016/j.ecss.2005.11.039>, 2006.
- Lyard, F. H., Allain, D. J., Cancet, M., Carrère, L., and Picot, N.: FES2014 global ocean tide atlas: design and performance, *Ocean Sci.*, 17, 615–649, <https://doi.org/10.5194/os-17-615-2021>, 2021.
- Marani, M., D'Alpaos, A., Lanzoni, S., Carniello, L., and Rinaldo, A.: The importance of being coupled: Stable states and catastrophic shifts in tidal biomorphodynamics, *J. Geophys. Res.-Earth*, 115, F04004, <https://doi.org/10.1029/2009JF001600>, 2010.
- Meadows, P., Meadows, A., and Murray, J.: Biological modifiers of marine benthic seascapes: Their role as ecosystem engineers, *Geomorphology*, 157, 31–48, <https://doi.org/10.1016/j.geomorph.2011.07.007>, 2012.
- Meyer, C. and Ragutski, G.: Forschungsbericht 21/1999 – KFKI Forschungsvorhaben Sedimentverteilung als Indikator für morphodynamische Prozesse MTK 0591, NLWKN Niedersachsen, [https://izw.baw.de/publikationen/kfki-projekte-berichte/0/048\\_2\\_1\\_e33603.pdf](https://izw.baw.de/publikationen/kfki-projekte-berichte/0/048_2_1_e33603.pdf) (last access: 19 April 2024), 1999.
- Meyer, J., Nehmer, P., and Kröncke, I.: Shifting south-eastern North Sea macrofauna bioturbation potential over the past three decades: A response to increasing SST and regionally decreasing food supply, *Mar. Ecol. Prog. Ser.*, 609, 17–32, 2019.
- Meysman, F., Middelburg, J., and Heip, C.: Bioturbation: a fresh look at Darwin's last idea, *Trends Ecol. Evol.*, 21, 688–695, <https://doi.org/10.1016/j.tree.2006.08.002>, 2007.
- Mitsch, W. J. and Gosselink, J. G.: *Wetlands*, John Wiley & Sons, New York, 582 pp., ISBN 978-1-118-67682-0, 2007.
- Mohr, V.: Modeling the Impact of Seagrass on Coastal Morphodynamics in a Tidal Basin, Master thesis, University of Hamburg, 2022.
- Montserrat, F., Van Colen, C., Degraer, S., Ysebaert, T., and Herman, P.: Benthic community-mediated sediment dynamics, *Mar. Ecol. Prog. Ser.*, 372, 43–59, <https://doi.org/10.3354/meps07769>, 2008.
- Murray, A. B., Knaapen, M., Tal, M., and Kirwan, M.: Biomorphodynamics: Physical-biological feedbacks that shape landscapes, *Water Resour. Res.*, 44, W11301, <https://doi.org/10.1029/2007WR006410>, 2008.
- Nasermoaddeli, M. H., Lemmen, C., Koesters, F., Stigge, G., Kerimoglu, O., Burchard, H., Klingbeil, K., Hofmeister, R., Kreuz, M., and Wirtz, K.: A model study on the large-scale effect of macrofauna on the suspended sediment concentration in a shallow shelf sea, *Estuar. Coast. Shelf S.*, 211, 62–76, <https://doi.org/10.1016/j.ecss.2017.11.002>, 2017.
- Oreskes, N., Shrader-Frechette, K., and Belitz, K.: Verification, Validation, and Confirmation of Numerical Models in the Earth Science, *Science*, 263, 641–646, <https://doi.org/10.1126/science.263.5147.641>, 1994.
- Orvain, F.: Modélisation de la bioturbation et de ses conséquences sur les flux de remise en suspension des sédiments cohésifs de la Baie de Marennes-Oleron, PhD thesis (unpublished), Université de La Rochelle, France, 192 pp., <https://theses.fr/2002LAROS092> (last access: 19 April 2024), 2002.
- Paarlberg, A. J., Knaapen, M., de Vries, M., Hulscher, S., and Wang, Z. B.: Biological influences on morphology and bed composition of an intertidal flat, *Estuar. Coast. Shelf S.*, 64, 577–590, <https://doi.org/10.1016/j.ecss.2005.04.008>, 2005.
- Pianosi, F., Beven, K., Freer, J., Hall, J., Rougier, J., Stephenson, D., and Wagener, T.: Sensitivity analysis of environmental models: A systematic review with practical workflow, *Environ. Modell. Softw.*, 79, 214–232, <https://doi.org/10.1016/j.envsoft.2016.02.008>, 2016.
- Pinto, L., Fortunato, A., Zhang, Y., Oliveira, A., and Sancho, F.: Development and validation of a three-dimensional morphodynamic modelling system for non-cohesive sediments, *Ocean Model.*, 57–58, 1–14, <https://doi.org/10.1016/j.ocemod.2012.08.005>, 2012.
- Plater, A. J. and Kirby, J. R.: 3.03 – Sea-Level Change and Coastal Geomorphic Response, *Treatise on Estuarine and Coastal Science*, 3, 39–72, <https://doi.org/10.1016/B978-0-12-374711-2.00304-1>, 2011.
- Pleskachevsky, A., Gayer, G., Horstmann, J., and Rosenthal, W.: Synergy of satellite remote sensing and numerical modelling for monitoring of suspended particulate matter, *Ocean Dynam.*, 55, 2–9, 2005.
- Potouroglou, M., Bull, J. C., Krauss, K. W., Kennedy, A. H., Fusi, M., Daffonchio, D., Mangora, M. M., Githaiga, M., Diele, K., and Huxham, M.: Measuring the role of seagrasses in regulating sediment surface elevation, *Sci. Rep.-UK*, 7, 11917, <https://doi.org/10.1038/s41598-017-12354-y>, 2017.
- Queirós, A., Birchenough, S., Bremner, J., Godbold, J., Parker, R., Romero-Ramirez, A., Reiss, H., Solan, M., Somerfield, P., Van Colen, C., Van Hoey, G., and Widdicombe, S.: A bioturbation classification of European marine infaunal invertebrates, *Ecol. Evol.*, 3, 3958–3985, 2013.
- Reeves, I. R. B., Moore, L. J., Goldstein, E. B., Murray, A. B., Carr, J. A., and Kirwan, M. L.: Impacts of seagrass dynamics on the coupled long-term evolution of barrier-marsh-bay systems, *J. Geophys. Res.-Biogeo.*, 125, e2019JG005416, <https://doi.org/10.1029/2019JG005416>, 2020.
- Reineck, H. E. and Singh, I.: Primary sedimentary structures in the recent sediments of the Jade, North Sea, *Mar. Geol.*, 5, 227–235, 1967.
- Reinhardt, L., Jerolmack, D., Cardinale, B., Vanacker, V., and Wright, J.: Dynamic Interactions of Life and its Landscape: Feedbacks at the Interface of Geomorphology and Ecology, *Earth Surf. Proc. Land.*, 35, 78–101, <https://doi.org/10.1002/esp.1912>, 2010.
- Reise, K., Herre, E., and Sturm, M.: Biomass and abundance of macrofauna in intertidal sediments of königshafen in the northern wadden Sea, *Helgolander Meeresun.*, 48, 201–215, <https://doi.org/10.1007/BF02367036>, 1994.
- Renaud, P., Niemi, A., Michel, C., Morata, N., Gosselin, M., Juul-Pedersen, T., and Chiuchio, A.: Seasonal variation in benthic community oxygen demand: A response to an ice algal bloom in the Beaufort Sea, Canadian Arctic?, *J. Marine Syst.*, 67, 1–12, <https://doi.org/10.1016/j.jmarsys.2006.07.006>, 2007.
- Ritzmann, A. and Baumberg, V.: Forschungsbericht 02/2013 – Oberflächensedimente des Jadebusens 2009: Kartierung anhand von Luftbildern und Bodenproben, NLWKN Niedersachsen, [https://www.nlwkn.niedersachsen.de/startseite/wasserwirtschaft/nordseekuste/forschungsstelle\\_kuste/morphologie/morphologie-38801.html](https://www.nlwkn.niedersachsen.de/startseite/wasserwirtschaft/nordseekuste/forschungsstelle_kuste/morphologie/morphologie-38801.html) (last access: 19 April 2024), 2013.

- Schückel, U. and Kröncke, I.: Temporal changes in intertidal macrofauna communities over eight decades: A result of eutrophication and climate change, *Estuar. Coast. Shelf S.*, 117, 210–218, <https://doi.org/10.1016/j.ecss.2012.11.008>, 2013.
- Schückel, U., Beck, M., and Kröncke, I.: Spatial distribution and structuring factors of subtidal macrofauna communities in the Wadden Sea (Jade Bay), *Mar. Biodivers.*, 45, 841–855, 2015a.
- Schückel, U., Kröncke, I., and Baird, D.: Linking long-term changes in trophic structure and function of an intertidal macrobenthic system to eutrophication and climate change using ecological network analysis, *Mar. Ecol. Prog. Ser.*, 536, 25–38, <https://doi.org/10.3354/meps11391>, 2015b.
- Schuurman, F., Marra, W. A., and Kleinhans, M. G.: Physics-based modeling of large braided sand-bed rivers: bar pattern formation, dynamics, and sensitivity. *J. Geophys. Res.-Earth*, 118, 2509–2527, 2013.
- Serrano, O., Arias-Ortiz, A., Duarte, C. M., Kendrick, G. A., and Lavery, P. S.: Impact of Marine Heatwaves on Seagrass Ecosystems, in: *Ecosystem Collapse and Climate Change, Ecological Studies*, vol. 241, edited by: Canadell, J. G. and Jackson, R. B., Springer, Cham, [https://doi.org/10.1007/978-3-030-71330-0\\_13](https://doi.org/10.1007/978-3-030-71330-0_13), 2021.
- Sievers, J., Rubel, M., and Milbradt, P.: EasyGSH-DB: Bathymetry (1996–2016), Bundesanstalt für Wasserbau [data set], <https://doi.org/10.48437/02.2020.K2.7000.0002>, 2020.
- Singer, A., Schückel, U., Beck, M., Bleich, O., Brumsack, H., Freund, H., Geimecke, C., Lettmann, K., Millat, G., Staneva, J., Vanselow, A., Westphal, H., Wolff, J., Wurpts, A., and Kröncke, I.: Small-scale benthos distribution modelling in a North Sea tidal basin in response to climatic and environmental changes (1970s–2009), *Mar. Ecol. Prog. Ser.*, 551, 13–30, <https://doi.org/10.3354/meps11756>, 2016.
- Skinner, C., Coulthard, T., Schwanghart, W., Van De Wiel, M., and Hancock, G.: Global sensitivity analysis of parameter uncertainty in landscape evolution models, *Universität Potsdam*, <https://doi.org/10.25932/publishup-46801>, 2018.
- Smith, C. R., Pope, R. H., DeMaster, D. J., and Magaard, L.: Age-dependent mixing of deep-sea sediments, *Geochim. Cosmochim. Ac.*, 57, 1473–1488, 1993.
- Stal, L.: Microphytobenthos as a biogeomorphological force in intertidal sediment stabilization, *Ecol. Eng.*, 36, 236–245, <https://doi.org/10.1016/j.ecoleng.2008.12.032>, 2010.
- Svenson, C., Ernsten, V., Winter, C., Bartholomä, A., and Hebbeln, D.: Tide-driven Sediment Variations on a Large Compound Dune in the Jade Tidal Inlet Channel, Southeastern North Sea, *J. Coastal Res.*, 56, 361–365, 2009.
- Umlauf, L. and Burchard, H.: A generic length-scale equation for geophysical turbulence models, *J. Mar. Res.*, 61, 235–265, 2003.
- US Army Corps of Engineers: Development of a Suspension Feeding and Deposit Feeding Benthos Model For Chesapeake Bay, <https://www.chesapeakebay.net/what/publications/development-of-a-suspension-feeding-and-deposit-feeding> (last access: 19 April 2024) 2000.
- Van Colen, C., Underwood, G., Serôdio, J., and Paterson, D.: Ecology of intertidal microbial biofilms: Mechanisms, patterns and future research needs, *J. Sea Res.*, 92, 2–5, <https://doi.org/10.1016/j.seares.2014.07.003>, 2014.
- Van der Wegen, M. and Roelvink, J. A.: Reproduction of estuarine bathymetry by means of a process-based model: Western Scheldt case study, the Netherlands, *Geomorphology*, 179, 152–167, 2012.
- Volkenborn, N. and Reise, K.: Lugworm exclusion experiment: Responses by deposit feeding worms to biogenic habitat transformations, *J. Exp. Mar. Biol. Ecol.*, 330, 169–179, 2006.
- Volkenborn, N., Robertson, D. M., and Reise, K.: Sediment destabilizing and stabilizing bio-engineers on tidal flats: cascading effects of experimental exclusion, *Helgolander Mar. Res.*, 63, 27–35, <https://doi.org/10.1007/s10152-008-0140-9>, 2009.
- Von Seggern, F.: Bestandsaufnahme in der Jade, *Hydrologische Untersuchungen, Wasserwirtschaftsamt, Wilhelmshaven*, p. 42, 1980.
- Waeles, B., Hir, P., and Silva Jacinto, R.: Modélisation morphodynamique cross-shore d'un estran vaseux, *C. R. Geosci.*, 336, 1025–1033, <https://doi.org/10.1016/j.crte.2004.03.011>, 2004.
- Waldock, C., Stuart-Smith, R., Albouy, C., Cheung, W., Edgar, G., Mouillot, D., Tjiputra, J., and Pellissier, L.: A quantitative review of abundance-based species distribution models, *CSH*, <https://doi.org/10.1101/2021.05.25.445591>, 2021.
- Walter, R. K., O'Leary, J. K., Vitousek, S., Taherkhani, M., Geraghty, C., and Kitajima, A.: Large-scale erosion driven by intertidal eelgrass loss in an estuarine environment, *Estuar. Coast. Shelf S.*, 243, 106910, <https://doi.org/10.1016/j.ecss.2020.106910>, 2020.
- Wang, C., Li, Q., Ge, F., Hu, Z., He, P., Chen, D., Xu, D., Wang, P., Zhang, Y., Zhang, L., Wu, Z., and Zhou, Q.: Responses of aquatic organisms downstream from WWTPs to disinfectants and their by-products during the COVID-19 pandemic, Wuhan, *Sci. Total Environ.*, 818, 151711, <https://doi.org/10.1016/j.scitotenv.2021.151711>, 2022.
- Weinert, M., Kröncke, I., Meyer, J., Mathis, M., Pohlmann, T., and Reiss, H.: Benthic ecosystem functioning under climate change: Modelling the bioturbation potential for benthic key species in the North Sea, *PeerJ*, 10, e14105, <https://doi.org/10.7717/peerj.14105>, 2022.
- Widdows, J. and Brinsley, M.: Impact of biotic and abiotic processes on sediment dynamics and the consequence to the structure and functioning of the intertidal zone, *J. Sea Res.*, 48, 143–156, [https://doi.org/10.1016/S1385-1101\(02\)00148-X](https://doi.org/10.1016/S1385-1101(02)00148-X), 2002.
- Wood, R. and Widdows, J.: A model of sediment transport over an intertidal transect, comparing the influences of biological and physical factors, *Limnol. Oceanogr.*, 47, 848–855, <https://doi.org/10.4319/lo.2002.47.3.0848>, 2002.
- Wrede, A., Dannheim, J., Gutow, L., and Brey, T.: Who really matters: influence of German Bight key bioturbators on biogeochemical cycling and sediment turnover, *J. Exp. Mar. Biol. Ecol.*, 488, 92–101, <https://doi.org/10.1016/j.jembe.2017.01.001>, 2017.
- WSV – Waterways and Shipping Authority Wilhelmshaven: Tide Gauge; WilhelmshavenTG, <https://emodnet.ec.europa.eu/geoviewer/> (last access: 1 April 2023), 2023.
- Zarnetske, P., Baiser, B., Strecker, A., Record, S., Belmaker, J., and Tuanmu, M. N.: The Interplay Between Landscape Structure and Biotic Interactions, *Current Landscape Ecology Reports*, 2, 12–29, <https://doi.org/10.1007/s40823-017-0021-5>, 2017.

- Zhang, W., Schneider, R., and Harff, J.: A multi-scale hybrid long-term morphodynamic model for wave-dominated coasts, *Geomorphology*, 149/150, 49–61, <https://doi.org/10.1016/j.geomorph.2012.01.019>, 2012.
- Zhang, W., Schneider, R., Kolb, J., Teichmann, T., Dudzinska-Nowak, J., Harff, J., and Hanebuth, T.: Land-sea interaction and morphogenesis of coastal foredunes – a modelling case study from the southern Baltic Sea coast, *Coast. Eng.*, 99, 148–166, <https://doi.org/10.1016/j.coastaleng.2015.03.005>, 2015.
- Zhang, Y. and Baptista, A.: SELFE: a Semi-implicit Eulerian-Lagrangian Finite-Element model for cross-scale ocean circulation, *Ocean Model.*, 21, 71–96, <https://doi.org/10.1016/j.ocemod.2007.11.005>, 2008.
- Zhang, Y., Ye, F., Stanev, E., and Grashorn, S.: Seamless cross-scale modelling with SCHISM, *Ocean Model.*, 102, 64–81, <https://doi.org/10.1016/j.ocemod.2016.05.002>, 2016.